Wind loads on low-slope roofs of buildings with large plan dimensions

by

Murad Aldoum and Ted Stathopoulos

Department of Building, Civil and Environmental Engineering, Concordia University, Montreal, Quebec, Canada

Abstract:

Wind load provisions in the North American codes and standards incorporate the results of wind tunnel studies and the full-scale measurements of wind loads. These studies examined wind effects on buildings with regular plan size, i.e. less than 60 m. This fact emphasizes the importance of testing large buildings in the wind tunnel and highlights the necessity of investigating the applicability of the North American code and standard provisions to large buildings. In the present study, three building models were constructed at a length scale of 1:400 with identical plan dimensions (equivalent to 118 m x 118 m) and different heights (equivalent to 5 m, 10 m and 20 m). The models were tested in simulated open country and suburban exposures. The experimental results were compared with full-scale data and the wind provisions of the North American codes and standards. It was found that the external peak pressure coefficients recommended by ASCE 7-16 [1] are much higher than the experimental findings whereas those recommended by ASCE 7-10 [2] are consistent with the experimental results. However, the experimental results indicate that the corner zone should be better defined as an L-shape for large buildings of 8 m height or more and the wind loads developed on the roof corner are approximately equal to those on the edge zone for large buildings of height less than 8 m.

Keywords: low-slope roof; large building; peak pressure coefficient; roof zonal system.

1 Introduction

Wind provisions in codes of practice and standards were established mainly based on testing building models in boundary layer wind tunnels. At the outset, wind effects on structures and machines were evaluated using aeronautical wind tunnels, whereas the idea of simulating wind flow in a boundary layer wind tunnel was first introduced by Jensen [3] in 1958. Jensen emphasized the need for more accurate simulation of the natural wind or the atmospheric boundary layer which can be accomplished by the simulation of turbulence intensities, spectra and probability distributions [4]. The study of wind effects on buildings in boundary layer wind tunnels was initiated effectively in the 1970s at Colorado State University and the University of Western Ontario. Results were published in many reports and papers, e.g., Akins and

Cermak [5], Peterka and Cermak [6], Davenport et al. [7], and Davenport et al. [8], and created the basic source for wind provisions in the North American codes and standards.

A high number of studies were conducted in boundary layer wind tunnels since the 70's. Stathopoulos and Surry [9] investigated the scaling effect on wind load measurements on low-rise buildings - this study concluded that a change in building model scale by a factor of 2 would result in a 10% error in the measured data. State-of-the-art papers and reviews of wind loads on low buildings have been published by many researchers, e.g., Stathopoulos [10], Holmes [11], Krishna [12], Kasperski [13] and Uematsu and Isyumov [14]. Stathopoulos [10] presented wind pressures measurement techniques and highlighted the important factors on wind loads and wind tunnel experiments, e.g., geometric scale, building height, terrain exposure…etc. Stathopoulos [15] studied the effect of pressure tap locations on roofs relative to the building edge on wind load measurements. The first row of pressure taps, unlike the location of taps in the conventional models, was very near to the leading edge (0.54 mm); the study concluded that the location of pressure taps with respect to the leading edge is very important and pressure coefficients measured for oblique wind direction on edge and corner zones are higher (in the order of 2 or 3) than those evaluated using models equipped with pressure taps in conventional locations.

Cochran and Cermak [16] conducted wind tunnel experiments on two models of Texas Tech University (TTU) experimental building in the wind tunnel of Colorado State University. The geometric scales used to construct the models were 1:50 and 1:100, and the resulted data were compared with full-scale measurements of the TTU experimental building. The results of this study showed that mean pressure coefficients measured on both models agree well with the full-scale data, however, discrepancies arise when the peak suction values are compared with the full-scale data. In addition, Cochran and Cermak [16] noted a reduction in peak suction pressures when the larger model (i.e. model of 1:50 length scale) is considered. Lin et al. [17] conducted wind tunnel experiments on five flat and nearly flat roof models, two of them are models of the TTU experimental building: one is a flat roof model, and the other is constructed with 1:60 (1/5:12) roof slope; moreover, all the models were constructed with a length scale of 1:50. The results of the study showed a very good agreement with full-scale data in the mean values of pressure coefficients, however, differences appear when comparing peak pressure coefficients with full-scale data.

Lin and Surry [18] studied the distribution of wind load on flat roofs of low-rise buildings. The study concluded that the size of roof pressure zones is independent of the plan dimensions of the building, and the size of the corner zone should be correlated to the height of the building, H. Also, pressure coefficients on the corner zone should be referred to tributary area normalized with respect to H^2. Furthermore, area-averaged pressure coefficients on the corner zone decrease to half beyond a tributary area of 0.1H X 0.1H.

Extensive experiments were carried out in the wind tunnel of the University of Western Ontario to enrich the aerodynamic database of the National Institute of Standards and Technology (NIST). The UWO contribution to the NIST aerodynamic database for wind loads on low buildings was published in three parts: part 1, Ho et al. [19], presents the aerodynamics data, part 2, St. Pierre et al. [20], includes comparisons with wind provisions in codes and standards, and part 3, Oh et al. [21], provides a detailed study about internal pressures.

Alrawashdeh and Stathopoulos [22] examined wind loads on square buildings with large configurations (i.e. more than 60 m). The study investigated the effect of wind on flat roof edges and corners of low-rise buildings with large plan dimensions. Nine building models were tested at the wind tunnel of Concordia University in a simulated open country exposure; each model was constructed at a length scale of 1:400 with a square flat roof and corresponding full-scale plan dimensions equal to 60 m, 120 m and 180 m. The experimental results of this study were compared with the American Society of Civil Engineers Standard (ASCE 7-10) [2], the National Building Code of Canada (NBCC 2010) [23], the European Standard (EN 1991-1-4, 2005) [24], and the Australian/New Zealand Standard (AS/NZS 1170.2, 2011) [25]. The study focused on the size of roof corner and edge zones and concluded that the size of corner and edge zones for large low-rise buildings of height less than 8 m should not be governed by the 4% of the least horizontal plan dimension but should be limited to 80% of the building height. Also, the study concluded that the external pressure coefficients in ASCE 7-10 [2] and NBCC 2010 [23] are adequate to be used in the design of large roofs of low-rise buildings.

Mooneghi et al. [26] studied wind loads on buildings with small heights using large models (i.e. length scales 1:6 and 1:5). The study used the partial turbulence simulation method to account for the missing low frequency components in the turbulence spectrum theoretically using quasi steady assumption. The results agree well with the full-scale data of the Silsoe cube and Texas Tech university experimental buildings.

Kopp and Morrison [27] examined component and cladding wind pressures on low-slope roofs of low-rise buildings focussing on the spatial distribution of wind pressures and the magnitude of pressure coefficients on roofs. The study investigated wind loads on many building models with low-slope roofs (less or equal to 1:12) in the boundary layer wind tunnel II at the University of Western Ontario under simulated open country and suburban exposures. In addition, experimental results acquired by Ho et al. [19] were used in this study, which concluded that the component and cladding external pressure coefficients recommended by ASCE 7-10 [2] for low-rise buildings with low-slope roofs are lower than the enveloped area-averaged pressure coefficients obtained by their wind tunnel experiments. In addition, the study showed that the size of pressure zones depends on the building height only, unlike ASCE 7-10 [2] provisions where the size of pressure zones is defined as a function of the height and the least plan dimension of the building.

Furthermore, the study recommended an L-shaped corner zone instead of the square corner zone in ASCE 7-10 [2]. The results of Kopp and Morrison [27] were adopted by ASCE 7 by increasing the magnitude of component and cladding external pressure coefficients of low-rise buildings with low-slope roofs, as well as, modifying the size and the shape of roof pressure zones for the same type of buildings in ASCE 7-16 [1].

Since all the studies considered in establishing the wind provisions in the North American codes and standards concerned only with buildings of regular size, their applicability to buildings of large geometries should be investigated. The objective of the present study is to investigate the applicability of wind provisions in ASCE 7-10 [2], ASCE 7-16 [1] and NBCC 2015 [28] to buildings of large roofs regarding the magnitude of peak pressure coefficients and the roof zonal system as well.

Wind effects were examined on the roof surface of three building models with similar square plan dimensions of 118 m and different heights: 5 m, 10 m and 20 m. The models were constructed using a length scale of 1:400 and tested in two simulated terrain exposures: open country and suburban for 7 wind directions, 0°- 90° with a step of 15°. The wind loads of the present study are presented in this paper as contours of most critical peak pressure coefficients among all wind directions; extreme mean and peak pressure coefficients for each wind azimuth; and area-averaged peak pressure coefficients as a function of tributary area. Also, comparisons with previous studies, full-scale data, and the provisions of North American codes and standards are included in this paper.

2 North American wind code and standard provisions

In North American codes and Standards, buildings can be classified in the low-rise category or mid-rise category according to the mean roof height of the building. Based on ASCE 7-10 [2] and ASCE 7-16 [1], a building is addressed as a low-rise building if the building height is less or equal 18.3 m (60 ft), whereas the height limit that separates the low-rise and mid-rise categories in NBCC 2015 [28] is 20 m (65.6 ft). Buildings of height greater than the mentioned limits are treated as mid-rise buildings. In fact, there is no clear upper limit for mid-rise buildings, although NBCC 2015 [29] considers buildings with 20 m < H < 60 m as mid-rise buildings for the design of main structural systems.

Wind loads specified by the North American codes and standards for low-slope roofs are provided for three or four pressure zones. Pressure zones divide the building roof into areas according to the variation of wind loads over the roof, high wind loads are assigned to areas close to the roof edges and corners and lower wind loads to interior areas. For low-rise buildings with low roof slope, ASCE 7-10 [2] and NBCC 2015 [28] provide similar roof zonal systems, see Fig. 1, where the size of corner and edge zones, z, depends on

building height and plan dimensions, such that "z is the lesser of 10% of the least horizontal dimension and 40% of height, but not less than 4% of the least horizontal dimension or 1 m" [28]. On the other hand, the zonal system of ASCE 7-16 [1] is independent of the plan dimensions, and the size of pressure zones is solely dependent on the building height, as shown in Fig. 1. ASCE 7-10 [2] and ASCE 7-16 [1] provide similar provisions for mid-rise buildings, and the corner zone has an L-shape and a size of 10% of the least horizontal dimension**,** D, see Fig. 2.

Based on ASCE 7-10 [2], ASCE 7-16 [1] and NBCC 2015 [28] and neglecting the internal pressures; design wind pressures are calculated according to Eqs. (1), (2) and (3), respectively.

$$P = \frac{1}{2}\rho V^2 K_z K_{zt} K_d G C_P \tag{1}$$

$$P = \frac{1}{2}\rho V^2 K_z K_{zt} K_d K_e G C_P \tag{2}$$

$$P = q I_w C_e C_t C_P C_g \tag{3}$$

where:

ρ: Air density

V : Basic wind velocity

K_z and C_e: Exposure factors

K_{zt} and C_t: Topographic factors

K_d: Directionality factor

K_e: Ground elevation factor

$q = \frac{1}{2}\rho V^2$: Velocity pressure

G and C_g: Gust factors

C_P: Mean pressure coefficient

GC_P and $C_P C_g$ refer to peak pressure coefficients in the North American codes, and wind loads for components and cladding are given in terms of peak pressure coefficients, more information about wind load factors and coefficients in codes is available in Davenport [30] and Stathopoulos [31]. Cladding and component peak pressure coefficients are presented in the codes as a function of tributary area, values

provided in ASCE 7-10 [2] and ASCE 7-16 [1] are based on velocity averaging time of 3 seconds, whereas peaks provided in NBCC 2015 [28] and the present study are based on 1 hr velocity averaging time.

Figs. 1 and 2 present cladding and component peak pressure coefficients of NBCC 2015 [28], ASCE 7-10 [2] and ASCE 7-16 [1] for roofs of low-rise and mid-rise buildings. Peaks of ASCE 7-10 [2] and ASCE 7-16 [1] were modified to be comparable with NBCC 2015 [28] and the experimental results of the present study by using mean hourly velocity pressure and considering the directionality effects. According to ASCE 7-10 [2] and ASCE 7-16 [1], directionality factor, K_d , is equal to 0.85 for the design of cladding and components of buildings, and based on the Durst curve, the ratio of the wind speed averaged over 3 seconds to the wind speed averaged over 1 hr is equal to 1.525. For example, maximum external peak pressure coefficient on zone 3 of ASCE 7-16 [1] is equal to -3.2, then, this coefficient should be multiplied by the directionality and the square of the velocity conversion factor as follows:

$$CpCg_{modified} = (1.525)^2 K_d CpCg_{ASCE\ 7}$$

$$CpCg_{modified} = (1.525)^2 \text{ x } 0.85 \text{ x } (-3.2) = -6.3$$

The 20 m high building is classified as a low-rise building according to NBCC 2015 [2/] (H ≤ 20 m). However, based on ASCE 7-10 [2] and ASCE 7-16 [1], the 20 m high building is a building with intermediate height. Fig. 3 shows mean pressure coefficients and pressure zones of NBCC 2015 [28] for buildings with heights greater than 20 m. For the design of cladding and components, the gust factor, Cg, in NBCC 2015 [28] is equal to 2.5.

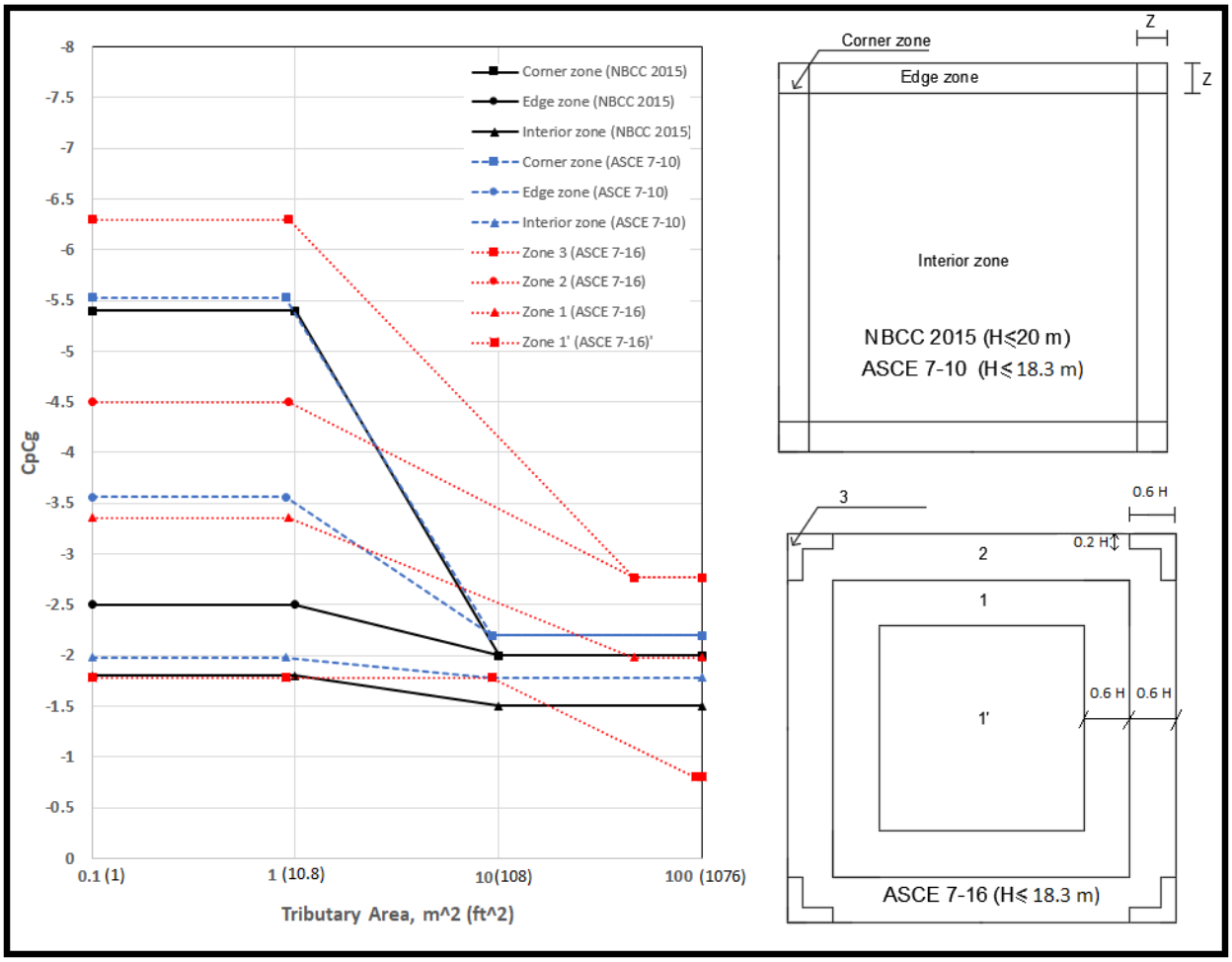

Figure 1: External peak pressure coefficients (NBCC format) and zonal systems of the North American codes and standards for low-slope roofs on low-rise buildings.

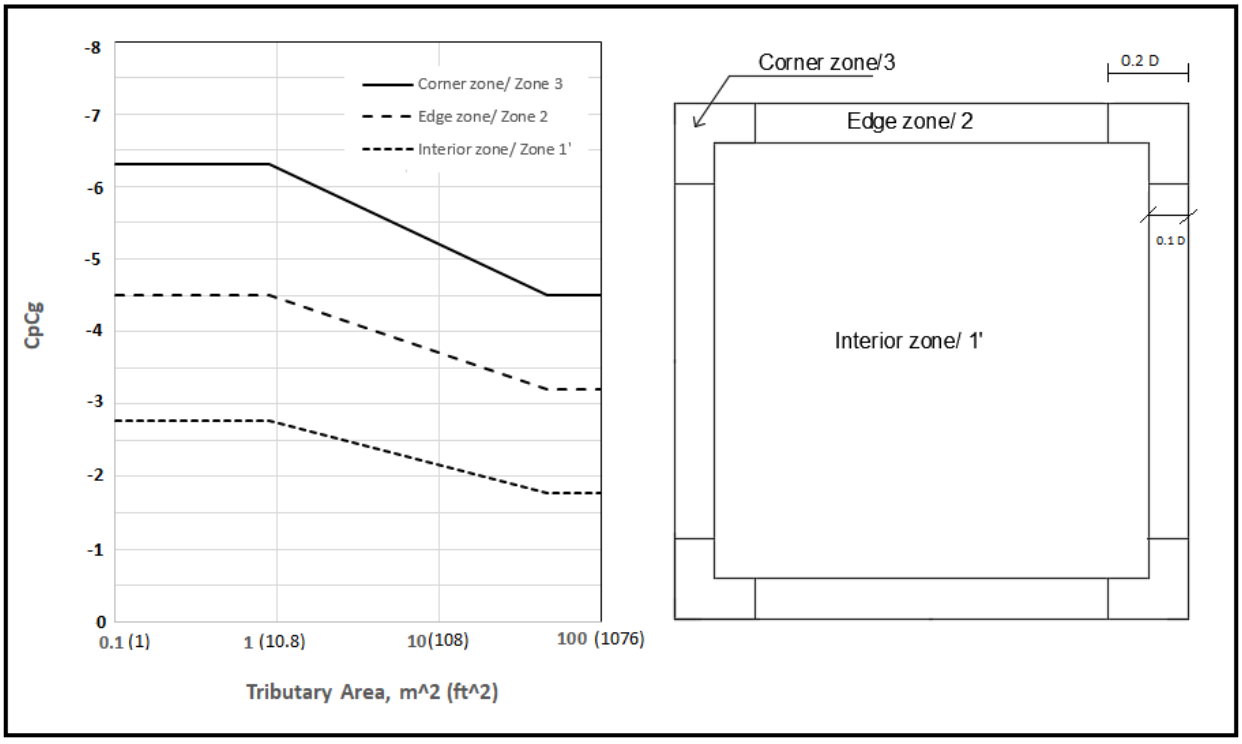

Figure 2: External peak pressure coefficients (NBCC format) and the zonal system of ASCE 7 for mid-rise buildings.

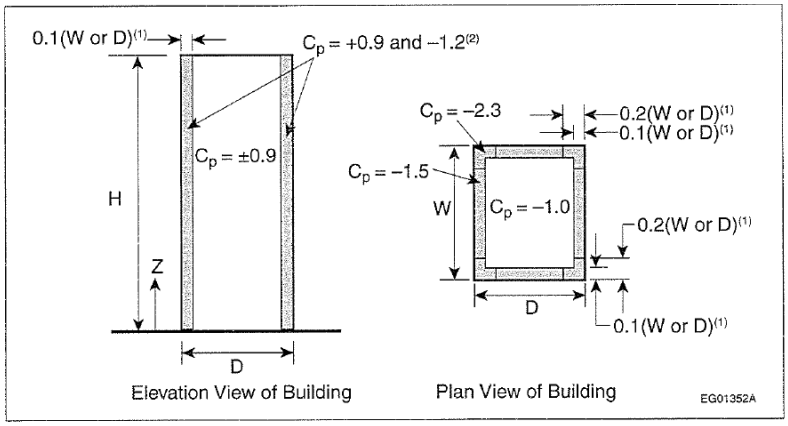

(1) The larger of W or D is to be used.
(2) Where vertical ribs deeper than 1 m are present on the walls, the dimensions 0.1D and 0.1W must be changed to 0.2D and 0.2W and the negative value of C_p must be changed from –1.2 to –1.4.

Figure 3: Values of Cp in NBCC 2015 [28] for a building height greater than 20 m on roof and walls for the design of structural components and cladding. (Figure A-4.1.7.5. (4) in NBCC 2015 [28]).

3 Experimental methodology

In this study, as mentioned previously, three nearly flat roof building models (roof angle of 1.4°) of similar full-scale plan dimensions of 118 m x 118 m were constructed at a geometric scale of 1:400, representing heights of 5 m, 10 m and 20 m. The experimental work of this study has been conducted in the boundary layer wind tunnel of the Building Aerodynamics Laboratory of Concordia University for two simulated terrain exposures: open country and suburban. It should be noted that open country and suburban exposures are referred to as exposure C and exposure B in ASCE 7-16 [1], and open terrain and rough terrain in NBCC 2015 [28], respectively.

The wind tunnel of Concordia University is an open return circuit wind tunnel. The tunnel is 12 m long which is adequate to acquire a properly simulated atmospheric boundary layer, and it has a width of 1.8 m and an adjustable height up to 1.8 m, also, the tunnel is equipped with a Mark Hot double inlet centrifugal blower to generate wind with a maximum speed of 14 m/s. The tunnel floor is basically furnished by a thick carpet to simulate terrain type of an open country exposure; other roughness elements with different configurations may be utilized for the simulation of other exposures, e.g. suburban [32]

Fig. 4 shows roof dimensions with pressure tap layout, as well as a detailed pressure tap assembly in the bottom-left quarter of the roof. The roof was equipped by 188 pressure taps in the bottom-left quarter with a high density in the roof corner and edges and with additional 6 pressure taps in the top-left corner. The first pressure taps line in both X and Y directions is 1 m from the roof edge, and the distribution of taps is the same along X and Y directions, therefore, the location of each pressure tap is presented in the vertical direction only. The results of this study are to be compared with full-scale measurements of the experimental building of Duro-Last Roofing, Inc. in Iowa [33]. The black pressure taps in the bottom-left quarter in Fig. 4(a) and the 6 pressure taps in the top-left corner represent the full-scale pressure tubes equipped in the roof of Duro-Last roofing experimental building.

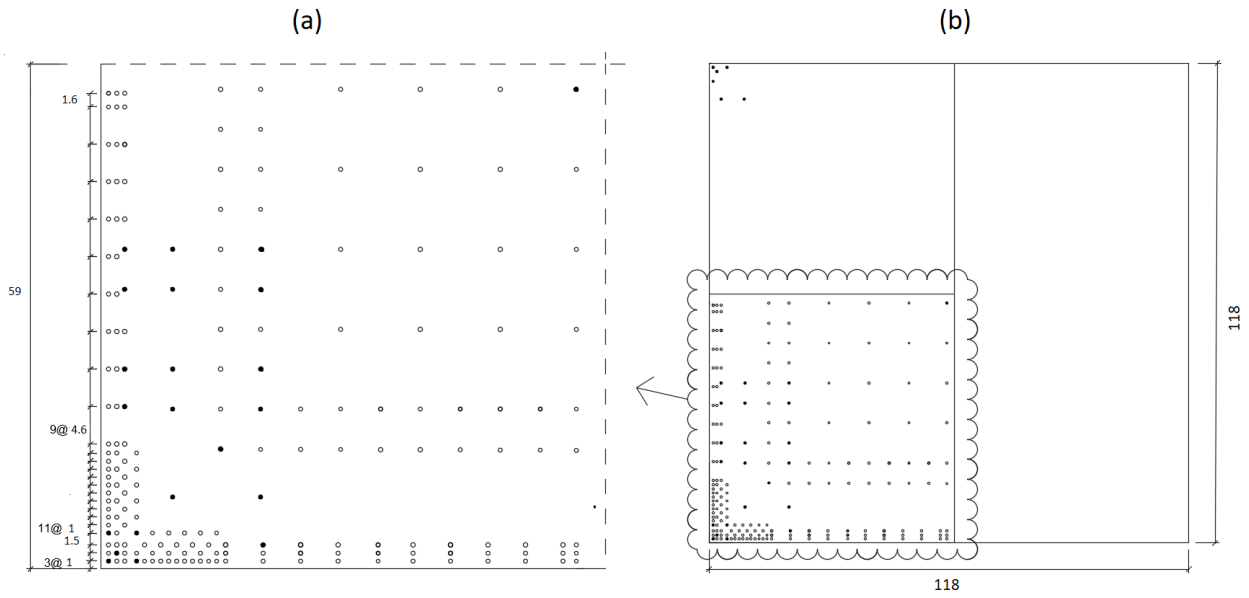

Figure 4: (a) Detailed pressure tap assembly with dimensions (m), (b) Roof plan dimensions (m) with pressure tap layout.

As shown in Fig 5, the wind tunnel floor was furnished with a carpet to simulate exposure C, while roughness elements, small foam cubes and eggboxes, were placed on the floor of the wind tunnel for the simulation of exposure B. Using a 4-hole cobra probe, variation of mean wind speed and turbulence intensity with height were measured at the wind tunnel and presented in Fig. 6 for both exposures. The power-law exponent was 0.14 for exposure C and 0.20 for exposure B, and the turbulence intensity was greater in suburban exposure.

Figure 5: Simulation of exposure C and exposure B at the wind tunnel of Concordia University.

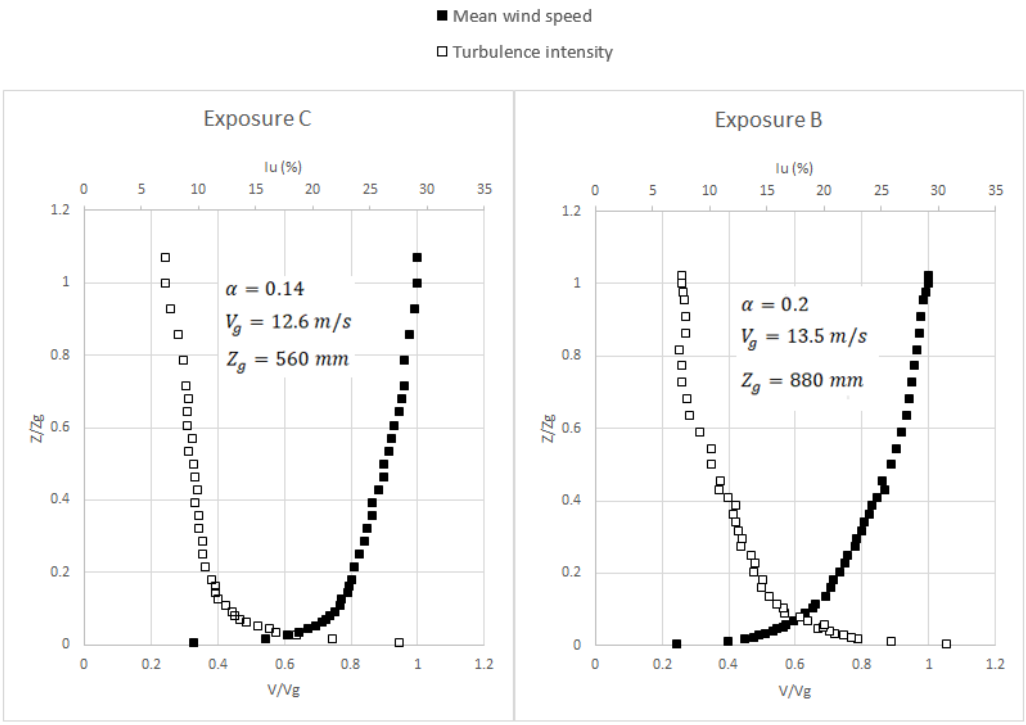

Figure 6: Vertical variation of mean wind speed and longitudinal turbulence intensity for exposure C and exposure B.

Results in this study are presented by using pressure coefficients, i.e., the well-known velocity-independent dimensionless parameters. The pressure coefficient can be defined as the wind-induced pressure (the difference between wind pressure and atmospheric pressure) normalized by the dynamic pressure at the eave height. The pressure coefficient (C_P) takes the following form:

$$C_P = \frac{\triangle P}{\frac{1}{2}\rho V^2} \tag{4}$$

where ρ is the air density ($1.255\ kg/m^3$) and V is the mean wind speed at the eave height. Pressure measurements were carried out in the wind tunnel using a pressure measurement system produced by Scanivalve Corporation. The measurements were performed for 7 wind directions: 0°, 15°, 30°, 45°, 60°, 75° and 90° and for two terrain exposures. The instantaneous pressures were measured at a frequency of 300 Hz for 27.3 seconds, which provides a time history of 8200 pressure readings for each pressure tap. Mean pressure coefficient (C_P) is the average value of 8200 readings. The peak values of pressure coefficients were calculated by using the well-known Gumbel-fitting method, with details described in [22]. It is important to mention that these peak values were determined with the same approach used previously for the evaluation of design pressure coefficients in the American and Canadian wind standards.

The pressure signals are transmitted from each pressure tap to the pressure scanners using two plastic tubes of around 30 cm in length, connected by a tiny brass pipe (restrictor), which works as a damper to eliminate resonance from the system. Also, the measurement system was designed to minimize phase shift and change in amplitude of the pressure signals.

Instantaneous area-averaged pressure coefficients $C_{P,A}(t)$ were measured on several areas in corner, edge and interior zones based on the following equation:

$$C_{P,A}(t) = \frac{\sum_{i=1}^{n} C_{Pi}(t) A_i}{\sum_{i=1}^{n} A_i} \tag{5}$$

where A_i is the tributary area of the ith pressure tap, n is the number of pressure taps in the considered area and $C_{Pi}(t)$ is the instantaneous pressure coefficient of ith pressure tap at instant t.

Based on the building height, the Reynolds number in the wind tunnel for the 5 m high building only is around 6,000, which is lower than the value of 11,000 recommended by ASCE 49-12 [34], the Wind Tunnel Testing for Buildings and other Structures Standard. This recommendation, although not explained in ASCE 49-12, originates from Nakamura and Ozono [35] recommending that this minimum value could be as low as 4,000 for high values of suction coefficients, i.e. precisely the design values that this study addresses. In addition, based on (3), ASCE 49-12 [34] also recommends the Jensen number similarity requirements, namely:

$$\left(\frac{L_b}{z_o}\right)_m = \left(\frac{L_b}{z_o}\right)_p \tag{6}$$

in which the model (m) and the prototype (p) ratios of the characteristic length (L_b) over the roughness length (z_o) are equal. Given that z_o is equal to 0.03 m for open terrain (Exposure C), as per ASCE 49-12 [34] and 0.08 mm in the wind tunnel, as per the measured velocity profile

$$\left(\frac{L_b}{z_o}\right)_p = \frac{5\text{m}}{0.03\text{m}} = 167 \quad \text{and} \quad \left(\frac{L_b}{z_o}\right)_{m(1:400)} = \frac{12.5\text{mm}}{0.08\text{mm}} = 156$$

showing an excellent similarity agreement. Similar results were obtained for Exposure B. Clearly, Jensen number would be violated for all building models if a larger geometric scale were used. In addition, the Reynolds number is sometimes calculated using the building width as for instance, in Geurts and Bentum [36]. This may be of particular interest in the present study, where buildings with very large horizontal dimensions are under consideration. Furthermore, changing the upstream terrain roughness to increase z_o and satisfy the Jensen number similarity would also alter the turbulence intensity at roof height, which is

another critical parameter for simulation of wind loads on low buildings. In addition, it would also change the exposure category of the upstream terrain.

In balance, it was decided to test all building models in the 1:400 geometric scale.

Fig. 7 presents the power spectral density of longitudinal turbulence component calculated at one-sixth of the gradient height for open country and suburban exposures in the wind tunnel, as well as, the power spectra evaluated based on Von Karman's and Davenport's models of turbulence in open country exposure at one-sixth of the gradient height. Experimental spectra normalized by the variance of the wind speed are close to those of the literature models. Furthermore, by using these spectra the full-scale equivalent integral length scale of turbulence is about 105 m, which fits well with the suggested value in ASCE 49-12 [34] of 110 m for Exposure C. This is an additional re-assurance regarding the selection of geometric scale in this study.

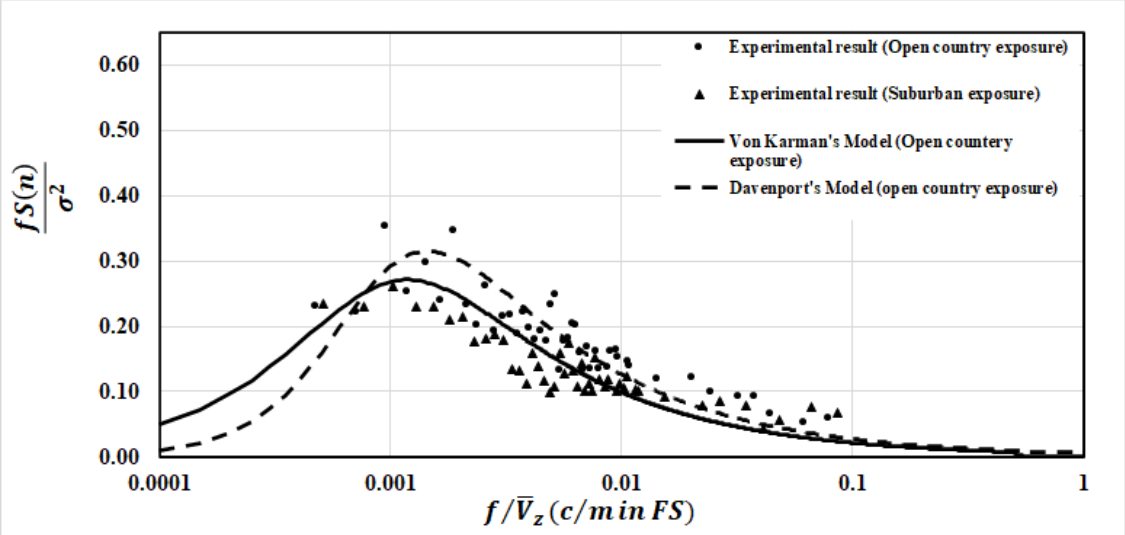

Figure 7: Power spectral density of longitudinal turbulence component evaluated at one-sixth of the gradient height.

4 Results and discussion

In this section, the experimental findings are presented in terms of extreme local pressure coefficients for each wind direction, contours of most critical peak pressure coefficients, and area-averaged peak pressure coefficients. The local and area-averaged mean and peak wind loads were evaluated in compliance with ASCE 49-12 [34].

4.1 Local pressure coefficients

Fig. 8 presents extreme (maximum) mean and peak pressure coefficients evaluated on the pressure zones of NBCC 2015 [28] and ASCE 7-10 [2] for each wind direction and for the 3 buildings in exposure C and exposure B. Although the building of 20 m height is classified as a low-rise building according to NBCC 2015 [28] ($H \leq 20$ m), it will be treated as mid-rise building because the height is at the boundary of low-rise building definition, further to the inadequacy of low-rise building provisions of NBCC 2015 [28] to cover the high wind loads on the building roof of 20 m height in the present study. Furthermore, a small relaxation in the geometric scale results in an error of the order of 10% for local and area wind loads [9]. Then, if the scale changes to 1:500, the biggest model would represent a building of height of 25 m instead of 20 m which means that the biggest model can reasonably simulate a mid-rise building.

As shown, the taller the building the larger the magnitude of wind pressure acting on its roof, which reflects the increased wind velocity pressure at the roof of the higher building. For instance, peak pressure coefficient, CpCg, on corner zone and at wind azimuth of 30° in exposure C is -7.4 for the 20 m high building and -4.1 for the 10 m high building, which results in a large difference of 3.3. On the other hand, the difference in pressure coefficients on the corner zone between the 10 m and 5 m high buildings is low and does not exceed 1 in the worst scenario. Values of peak and mean pressure coefficients on the edge zone of the building of 20 m height are lower than those of the other two low-rise buildings, 10 m and 5 m high. Further, pressure coefficients developed on the edge zone of the 5 m high building are somewhat higher than those of the 10 m high building.

For the interior zone, peak and mean pressure coefficient are lower compared to those of the corner and the edge zones, and the wind pressure coefficients are higher for the taller building.

With the exception of the 5 m high building, most critical pressure coefficients, among all wind directions, on corner zone were recorded at wind directions ranging from 15° to 30° or 60° to 75°. However, the most critical wind loads on the roof of the 5 m high building occur at normal wind directions. It should be noted that values of pressure coefficients for wind directions from 0° to 45° are not equal to those for wind direction from 45° to 90°. This is probably due to the small roof slope (1.4°) and the small margin of experimental error. In addition, there is also some asymmetric wind speed distribution with respect to the centerline of the testing area in the wind tunnel but the error in this regard does not exceed 5% [32].

Mean pressure coefficients are similar in both terrain exposures, while peak pressure coefficients in suburban exposure are higher which reflects the increased gustiness in the rougher exposure. It is very important to realize that the higher peak pressure coefficients evaluated in exposure B do not reflect necessarily higher wind pressures developed on the roof due to the lower wind speed at the mean roof

height in the rougher terrain. In fact, codes and standards provide lower design pressures for buildings in exposure B compared to those provided for buildings immersed in exposure C by considering higher exposure factors for wind load estimation on buildings in exposure C. For instance, according to ASCE 7 and for a building of 4.9 m (16 ft) height, the exposure factor K_Z is 0.883 and 0.585 for exposure C and exposure B, respectively.

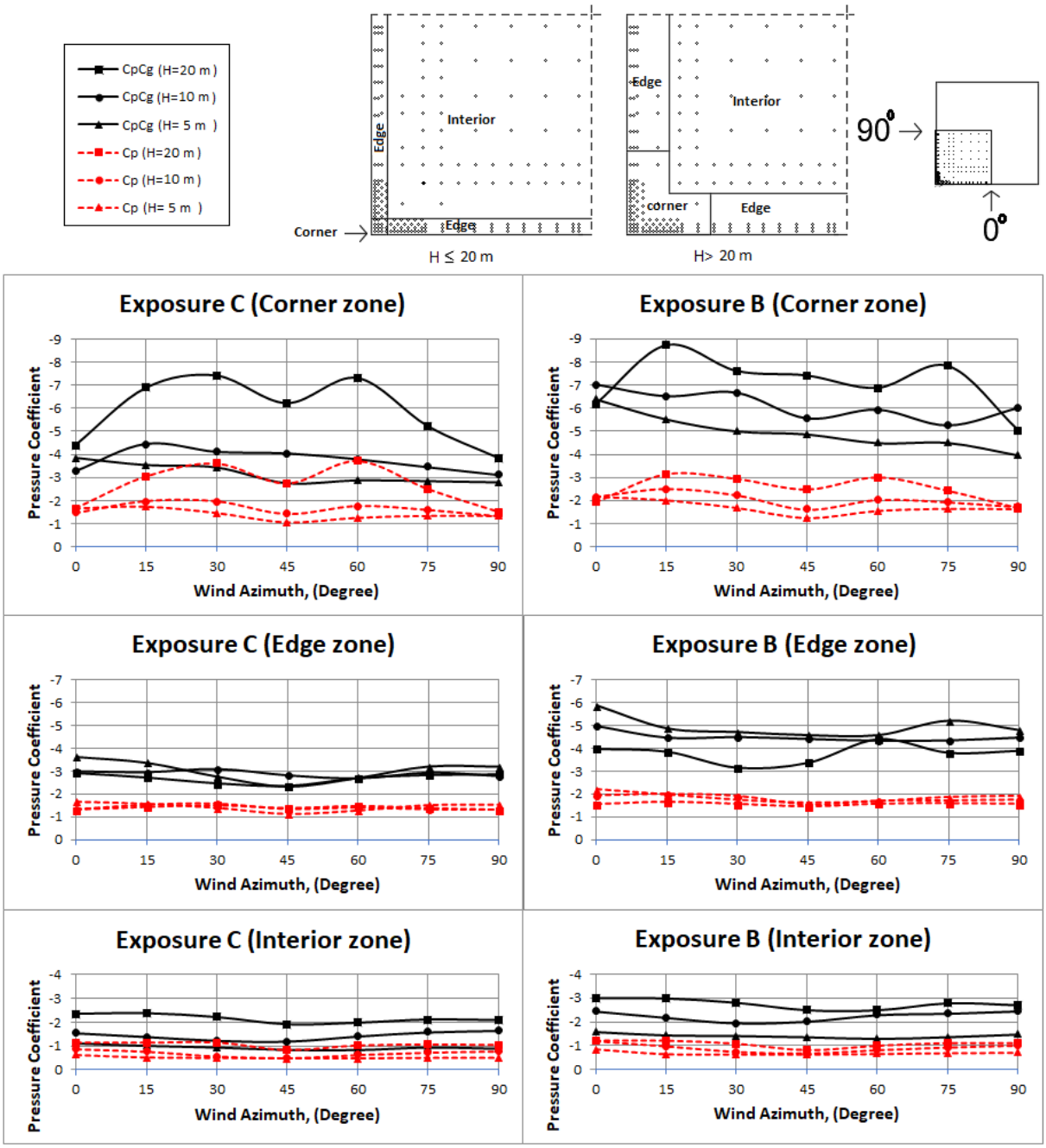

Figure 8: Extreme peak and mean pressure coefficients on the pressure zones defined by ASCE 7-10 [2] and NBCC 2015 [28] versus wind direction for 3 different heights and two exposures.

4.2 Contours of most critical peak pressure coefficients

The building models have been tested for 7 wind directions: 0°, 15°, 30°, 45°, 60°, 75°, and 90° to obtain the most critical peak pressure coefficients on the roof of the buildings. Fig. 9 shows contours of most critical peak pressure coefficients among all wind directions for three heights in exposure C. The contours show wind pressure coefficients within the bottom-left quarter of the roof, which is the area equipped with pressure taps. All contours were created by the mapping software "surfer 15" with a contour interval of 0.5.

As shown in the figure, and except for the 5 m high building, pressure coefficients decrease from the highest value on the roof corner to relatively smaller values along both windward edges up to the middle of the windward edge, beyond which, pressure coefficients increase to reach the highest value on the other corner of the roof. However, for the 5 m high building, wind loads developed on corner and edge zones are comparable.

Pressure coefficients decrease from the windward edge toward the interior zone along a line normal to the windward edges. This is so, because of the flow separation at the windward edges causing high wind pressures on corner and edge zones compared to those on the interior zone.

Height is a significant factor that affects the value of pressure coefficients, as well as, the area at which the maximum pressure coefficients extend on the roof. Clearly, the taller the building the higher the pressure coefficients and the larger the area that receives high wind pressures.

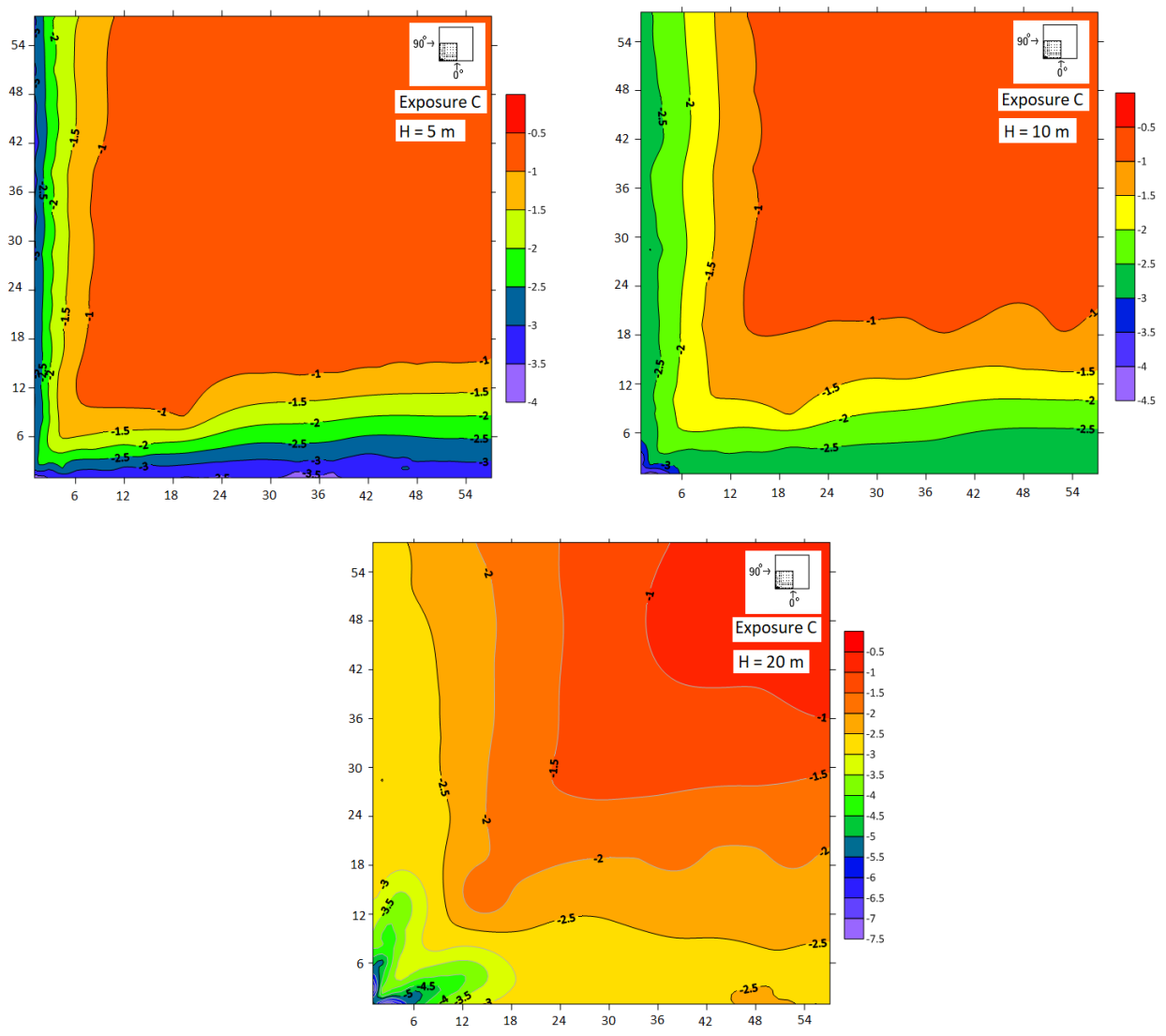

Figure 9: Most critical peak pressure coefficients (CpCg) among all wind directions on the roof of the three buildings in exposure C.

4.3 Area-averaged peak pressure coefficients

Design of cladding and components against wind loads depends on the area loads rather than the point loads, because when the wind loads exert on the façade or the roof of a building, it is resisted by an entire single component, such as an aluminum cladding panel. This requires the evaluation of the area-averaged wind loads in order to obtain accurate design pressures for the components and cladding with different areas. Wind loads are presented as a function of the tributary (effective) area in wind codes and standards. The area-averaged peak pressure coefficients on small areas are greater in magnitude than those on large areas.

Area-averaged wind pressure coefficients were evaluated for numerous tributary areas on the roof surface. Each tributary area represents the area associated with each pressure tap or a combination of two or more pressure taps. Area-averaged peak pressure coefficients are presented in the NBCC format. Fig. 10 shows the enveloped local and area-averaged peak pressure coefficients versus tributary area on corner, edge and interior zones for buildings of 5 m and 10 m heights in exposure C. Values of area-averaged peak pressure coefficients decrease as the tributary area increases in the corner zone, while the reduction in the values of area-averaged coefficients with the tributary is smaller in the edge zone. Also, the experimental results show that the reduction of area-averaged wind loads is very small over the tributary areas in the interior zone. Fig. 11 shows the most critical local and area-averaged peak pressure coefficients for the 20 m high building - results exhibit the same trend as in Fig.10. Area-averaged peaks evaluated for exposure B showed the same trends as in Figs. 10 and 11.

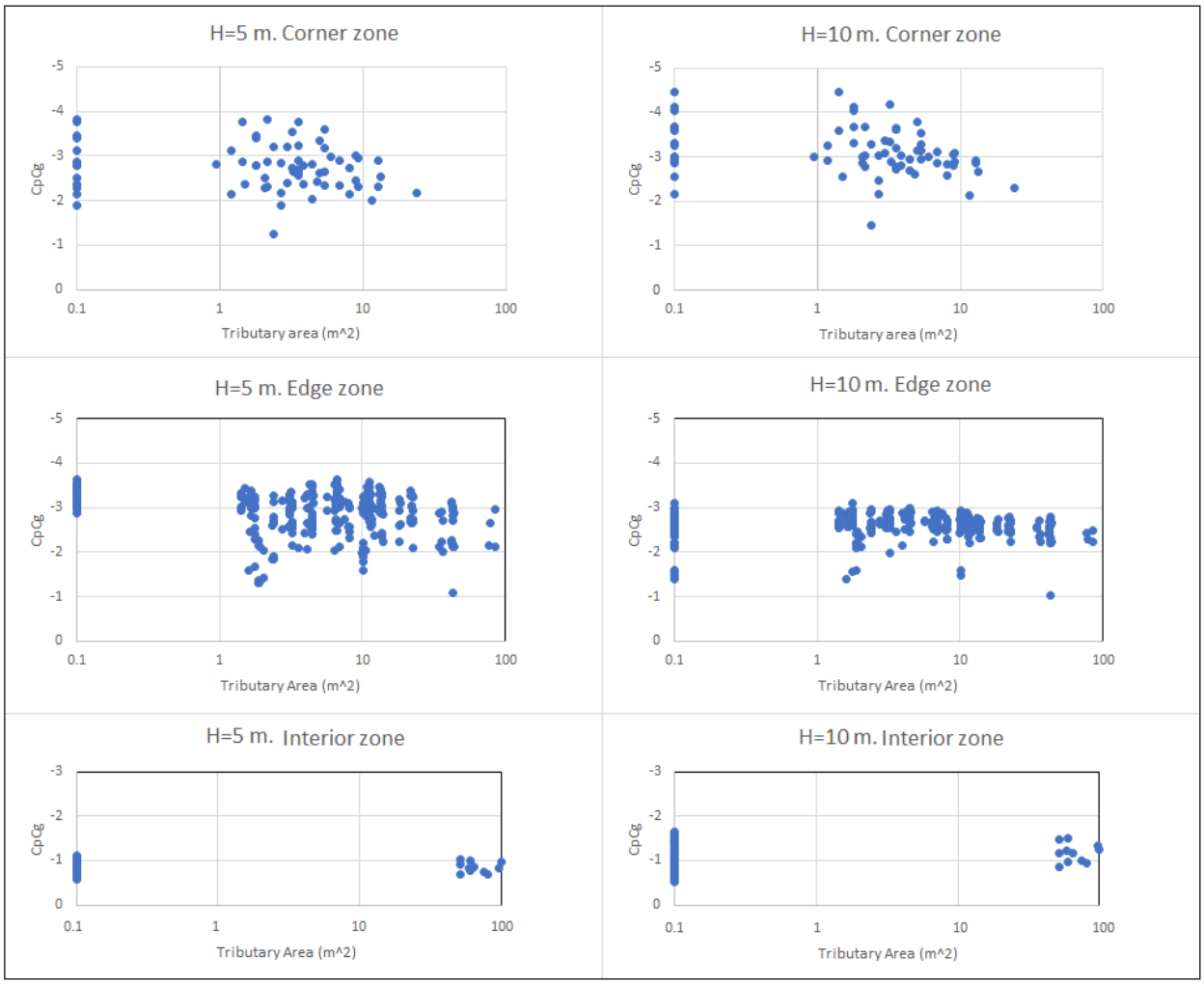

Figure 10: Most critical local and area-averaged peak pressure coefficients for all wind directions on pressure zones defined by ASCE 7-10 [2] and NBCC 2015 [28] for buildings of 5 m and 10 m heights – exposure C

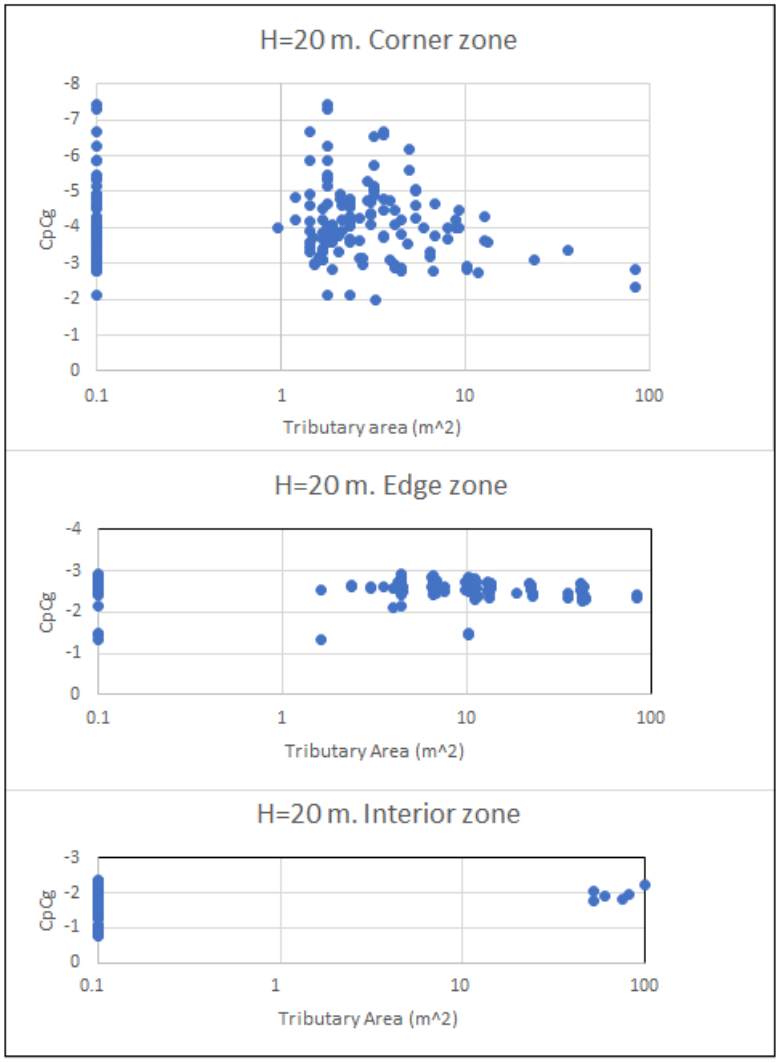

Figure 11: Most critical local and area-averaged peak pressure coefficients for all wind directions on pressure zones defined by NBCC 2015 [28], ASCE 7-10 [2] and ASCE 7-16 [1] for buildings of 20 m height – exposure C.

5 Previous work

Alrawashdeh and Stathopoulos [22] investigated wind loads on large low buildings. The results of the 10 m high building in the present study in exposure C have been compared with the results of the corresponding building (120 m x 120 m x 10 m) in [2] – see Fig. 12.

Fig. 12(a) shows the variation of peak and mean pressure coefficients along the centerline of the roof for 0° wind direction. Results of both studies are very close except the peak coefficient value of the pressure tap near the leading edge.

Fig. 12(b) shows the variation of peak and mean pressure coefficients along the line at the concurrent edge (X/B = 0.01) for 45° wind direction. Small discrepancies appear in the values of peak pressure coefficients along the entire line and the values of mean pressure coefficients near the leading edge (Y/L < 0.1). This is attributed to the different number and locations of pressure taps in this area accentuated by the conical vortices developed along the edge when the wind strikes at an azimuth of 45°. However, the values of mean pressure coefficients show a good agreement beyond Y/L = 0.1.

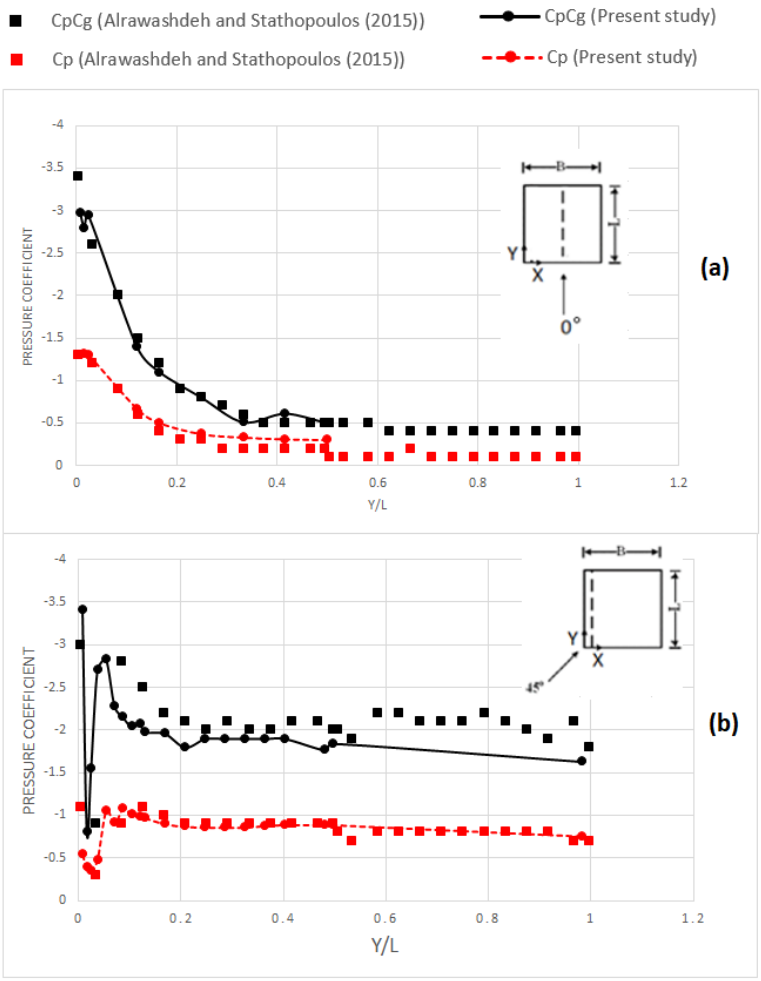

Figure 12: Comparison between the present study and Alrawashdeh and Stathopoulos [22],

(a) Variation of wind pressure coefficients along the roof centerline for 0° wind direction; and

(b) Variation in wind pressure coefficients along the line at the concurrent edge for 45° wind direction.

6 Comparison with full-scale data

The results of the present study were also compared with full-scale pressure measurement data from the roof of the experimental building of Duro-Last Roofing Inc. in Iowa site [33]. Fig. 13 shows a photo of the experimental building site captured from Google Earth. The experimental building was made available for full-scale measurements of wind pressures and speeds to investigate the new low-slope roof low-rise buildings provisions of ASCE 7-16 [1]. As shown in Fig. 14, the experimental building has plan dimensions of 73 m X 73 m (240 ft X 240 ft), eave height of 6 m (20 ft), and 1.4° roof slope. The roof of the experimental building is equipped with 28 pressure taps, 6 taps in the top-left roof corner and the rest in the bottom-left quarter. Fig. 14 (a) presents a detailed layout of the pressure taps on the bottom-left quarter of the roof, the quarter is divided into 4 pressure zones: zone 3, 2, 1 and 1', as defined in ASCE 7-16 [1]. Two anemometers are utilized to measure the wind speed in the site: one is fixed beside the building at a height of 8 m (26 ft) above the ground, and the other is installed above the building at a height of 11.6 m (38 ft) from the ground level. Moreover, the terrain exposure of the surrounding area near the experimental building can be classified as an open country exposure (exposure C).

Figure 13: The experimental building of Duro-Last Roofing Inc. in Iowa (Google Earth).

The experimental building model was equipped with 196 pressure taps and tested in the wind tunnel in a simulated open country exposure. As shown previously in Fig. 4, the black pressure taps in the bottom-left quarter and the 6 pressure taps in the top-left corner represent the full-scale pressure taps in the Duro-Last Roofing Inc. experimental building.

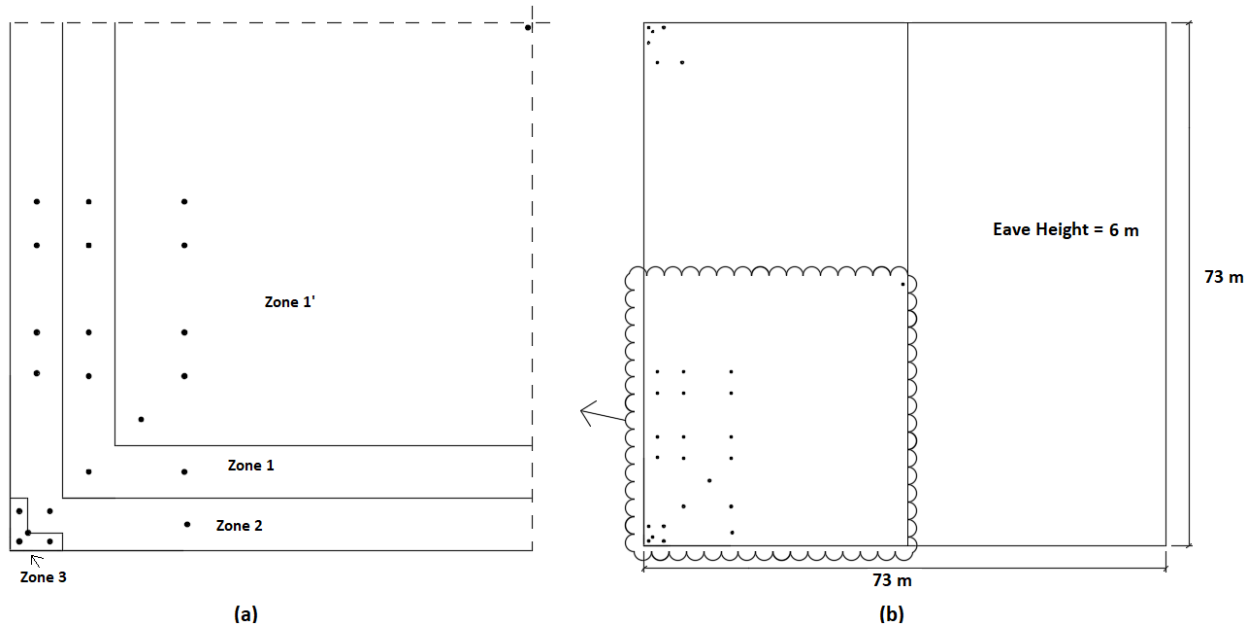

Figure 14: The experimental building of Duro-Last Roofing Inc. (a) Detailed pressure tap assembly, (b) Roof plan dimensions with pressure tap layout.

The full-scale peak pressure coefficients were calculated based on pressure measurements recorded at wind speed more than 15.6 m/s (35 mph). Fig. 15 presents the full-scale maximum, average and minimum peak pressure coefficients versus wind direction, as well as, the wind tunnel results based on the pressure records of the pressure taps corresponding to the full-scale pressure tubes. The full-scale peak pressure coefficients are presented for 3 wind directions: 0°, 90° and 135°. All peak pressure coefficients are presented in the format of ASCE 7, which is based on a velocity averaging time of 3 seconds.

The results of the present study are in a good agreement with the average full-scale peak pressure coefficients in zone 3 and zone 1 except at wind direction of 135° in zone 1, at which the peak pressure coefficient of the present study coincides with the minimum full-scale peak. In zone 1', however, the peak pressure coefficients of the present study are somewhat higher or lower than the minimum peak pressure coefficients of the full-scale measurements.

Fig. 16 shows the enveloped peak pressure coefficients of the full-scale data and the experimental results among three wind directions: 0°, 90° and 135° in the pressure zones of ASCE 7-16 [1]. The enveloped

wind tunnel peaks show a perfect agreement with the enveloped average full-scale peak pressure coefficient in zone 3, zone 2 and zone 1; while it is closer to the minimum enveloped full-scale peak in zone 1'.

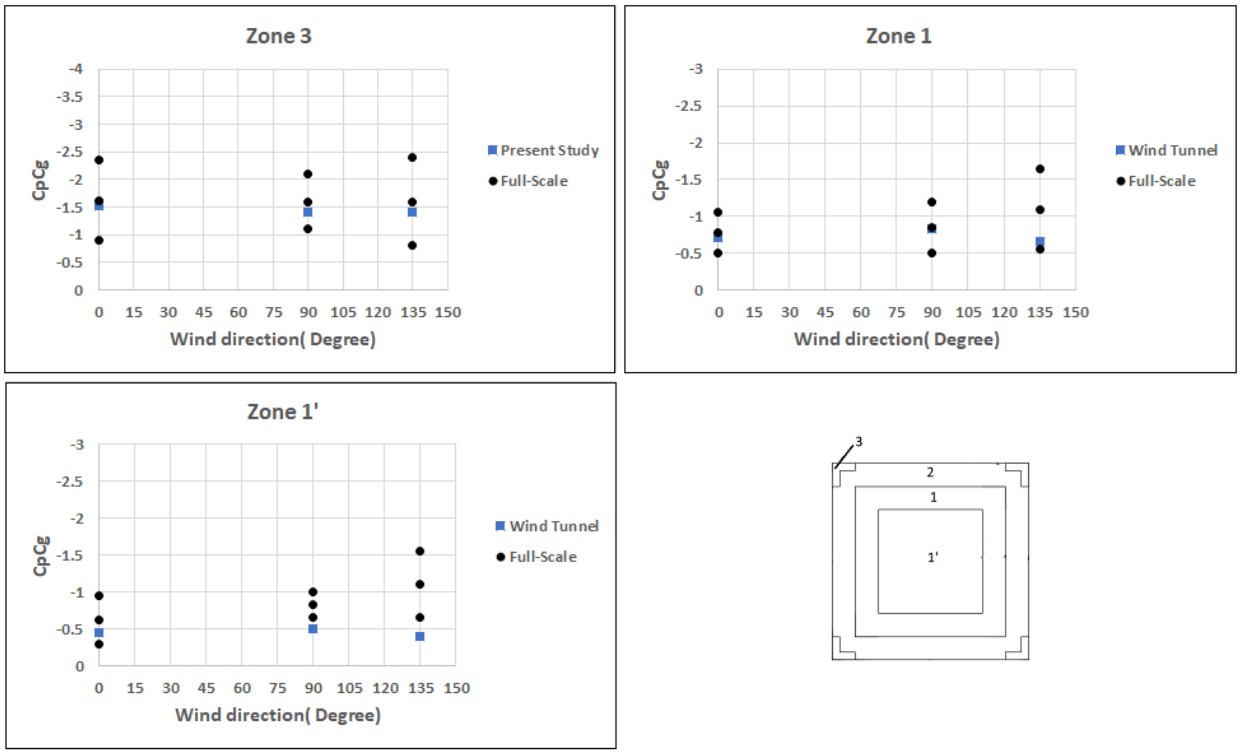

Figure 15: Comparison of extreme and peak pressure coefficients versus wind direction for zone 3, zone 1, and zone 1' between the results of the present study and the full-scale data measured on the experimental building of Duro-Last Roofing, Inc.

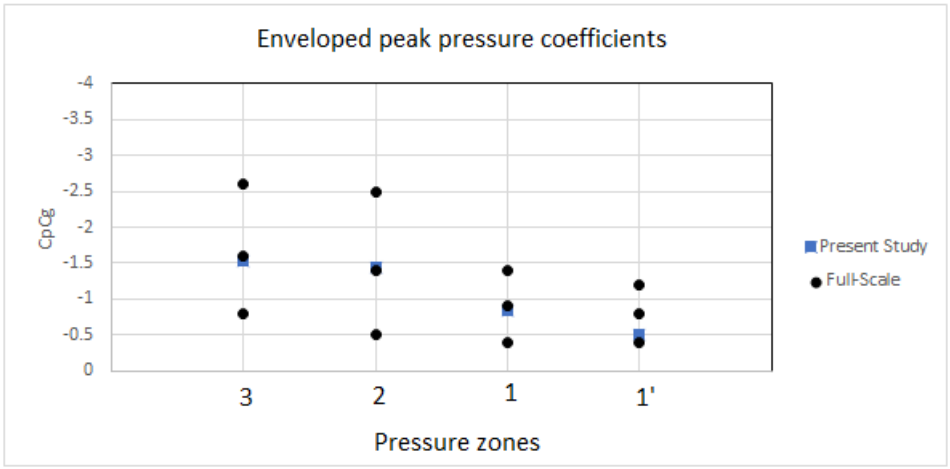

Figure 16: Comparison of the enveloped peak pressure coefficients between the full-scale data and the present study in ASCE 7 roof pressure zones.

7 Comparison with the North American codes

The experimental findings of the present study were compared with the wind provisions of the North American codes and standards to investigate their applicability to provide a convenient design for buildings of large geometries. The comparison was implemented in two regards: peak pressure coefficients on roof pressure zones and roof zonal systems.

7.1 Peak pressure coefficients

Local and area-averaged peak pressure coefficients of the present study were compared with the corresponding peaks provided by the North American codes and standards to examine the suitability of wind loads specified by the codes to provide safe and economical design for large roofs.

Since the present study examines wind loads for three heights, 5 m, 10 m and 20 m, the peaks provided by the codes should be modified to be comparable with the results of each building by considering the exposure factor. For instance, the external peak pressure coefficients for zone 3 in ASCE 7-16 [1] is equal to -6.3, see Fig. 2, and the exposure factor, K_z, of the building of 20 m height is equal to 1.16, then, the final value of the peak pressure coefficient specified by ASCE 7-16 [1] for the 20 m high building becomes -7.3. Table 1 summarises the exposure factors for the three buildings according to NBCC 2015 [28], ASCE 7-10 [2] and ASCE 7-16 [1] in exposure C.

Table 1: Exposure factors for the three buildings in the present study in exposure C.

Building height (m)	(C_e), NBCC 2015 [28]	(K_z), ASCE 7-10/16
5	0.9	0.88
10	1.01	1.01
20	1.15	1.16

7.1.1 Local pressure coefficients

As mentioned previously, external peak pressure coefficients recommended by NBCC and ASCE 7 are provided as area-averaged peak pressure coefficients, such that the maximum (in an absolute sense) external peak pressure coefficients are assigned for the minimum tributary areas (less than 1 m^2), and then, the external pressure coefficients attenuate to reach the minimum value for larger tributary areas. In this section, the most critical local pressure coefficients of the present study will be compared with the code external peak pressure coefficients corresponding to the minimum tributary area (i.e. 1 m^2) in each pressure zone.

Fig. 17 shows comparisons between the most critical peak pressure coefficients, CpCg, among all wind directions for the three buildings in the present study and the peaks recommended by the codes. Peak pressure coefficients of the 5 m high building are lower than values of external pressure coefficients specified by NBCC 2015 [28] and ASCE 7-10 [2] in the corner and the interior zones. However, in the edge zone, values of peak pressure coefficients of NBCC 2015 [28] and ASCE 7-10 [2] are exceeded by the experimental peak. Peak pressure coefficients of the new edition of the American standard, ASCE 7-16 [1], are higher than the experimental results in all pressure zones with a difference reaching 1.7 in the corner zone. This results in an overestimation of the design loads on large roofs and leads to overdesign and extra cost. The experimental results of the 5 m high building showed that similar peak pressure coefficients were recorded on the corner zone and the edge zone, which contrasts the recommendation of ASCE 7 and NBCC at which the peak pressure coefficients specified for the corner zone are higher than those for the edge zone.

For the building of 10 m height, values provided by the three codes are higher than the experimental peaks in all zones, except the peak pressure coefficient recommended by NBCC 2015 [28] for the edge zone, which is lower than the experimental findings of the present study. Therefore, the value of peak pressure coefficient recommended by NBCC 2015 [28] for areas less than $1\ m^2$ should be increased to match ASCE 7-10 [2] (from -2.5 to -3.6). Again, values of external pressure coefficients of ASCE 7-16 [1] are much higher than the experimental results, with a difference of 1.9 in the corner zone.

The bottom graph in Fig. 17 shows a comparison between the results of the present study for the 20 m high building and the provisions of the North American codes and standards. Both ASCE 7-16 [1] and ASCE 7-10 [2] provide the same external peak pressure coefficients and pressure zones for buildings of heights more than 60 ft. The experimental peak pressure coefficient evaluated on the corner zone is approximately equal to the peak pressure coefficient of ASCE 7-10 [2] and ASCE 7-16 [1], whereas the peak pressure coefficients of the same codes are higher than the experimental peak pressure coefficients calculated on the edge and the interior zones with a high difference of 2.3 for the edge zone. As mentioned previously, when the building height is less than 20 m, then it is considered as low-rise building based on NBCC 2015 [28]. The 20 m high building is at the limit, and for this reason, values of most critical peak pressure coefficients evaluated on its roof have been compared with the provisions of NBCC 2015 [28] for low-rise buildings and mid-rise buildings. As shown in the figure, the values of experimental peak pressure coefficients are significantly higher than those specified for low-rise buildings in NBCC 2015 [28]. On the other hand, the peak pressure coefficients of NBCC 2015 [28] for mid-rise buildings are greater than the experimental results, except for the corner zone, where the difference is relatively small. Clearly, for a

large building of height close to 20 m, it is recommended to consider the provisions of the mid-rise buildings.

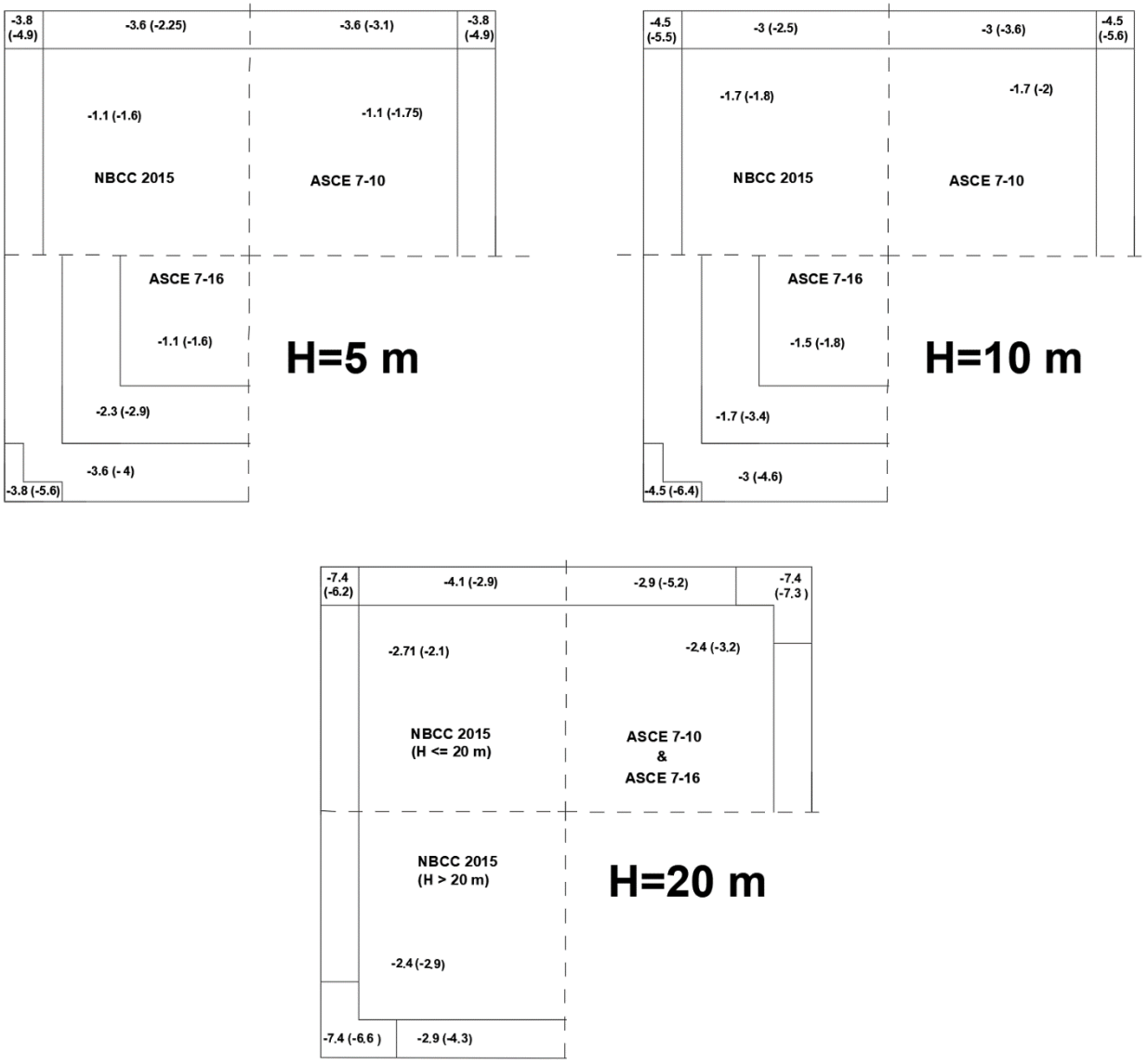

Figure 17: Comparison of most critical peak pressure coefficients between the present study for the three buildings in open country exposure and the corresponding recommended peaks of NBCC 2015 [28], ASCE 7-10 [2] and ASCE 7-16 [1]. (coefficients between brackets are the values recommended by NBCC 2015 [28] and ASCE 7-10/16).

7.1.2 Area-averaged peak pressure coefficients

Since the wind loads are presented as a function of tributary area, it is very important to compare the experimental area-averaged peaks with those specified by the North American codes and standards in order to assess the suitability of area-averaged peak pressure coefficients of the North American codes and standards to provide safe and economical design for large roofs. Figs. 18, 19 and 20 present comparisons

between the local and area-averaged peak pressure coefficients of the present study and those provided by NBCC 2015 [28], ASCE 7-10 [2] and ASCE 7-16 [1] in exposure C.

As shown in Figs. 18 and 19, the experimental area-averaged peaks evaluated on the edge zone of the 5 m high building are higher than those specified by NBCC 2015 [28] and ASCE 7-10 [2], while they are higher than the peak pressure coefficients provided by NBCC 2015 [28] only for the 10 m high building.

The experimental peaks recorded on some areas in the edge zone of the 5 m high building are similar in magnitude to those recorded in the corner zone, and the exact location of these areas at which the highest wind loads occur in the edge zone could not be determined. However, the codes recommend lower pressure coefficients for the edge zone, and to ensure a safe design for the components and cladding of the edge zone of this building, the recommended design peak pressure coefficients for the edge zone should be raised to be comparable to those recommended for the corner zone. This indeed will be very expensive for large buildings, but it is the only way to provide a safe design for the edge zone. On the other hand, area-averaged peaks of NBCC 2015 [28] and ASCE 7-10 [2] are higher than the experimental results in the corner and the interior zones for the buildings of 5 m and 10 m heights.

Peaks of ASCE 7-16 [1] are higher than the experimental results with a large difference in all pressure zones except in the corner zone of the 20 m high building where the ASCE 7-16 [1] peak is somewhat lower than the experimental peak, also, in the edge zone of the 5 m high building at large tributary areas. Again, the values of external peak pressure coefficients provided by ASCE 7-16 [1] for low-slope roofs of low-rise buildings are very conservative and result in a costly design for large roofs.

As already stated, area-averaged peak pressure coefficients decrease with the tributary area in the corner zones. In addition, the reduction in experimental area-averaged peak pressure coefficients with the tributary area in the interior zone agrees with the values specified by the codes for the interior zone at which the area-averaged peak pressure coefficients decrease marginally as the tributary area increases.

Moreover, it should be noted that the tributary area which corresponds to the minimum area-averaged peak pressure coefficients has been increased to be $46\ m^2$ $(500\ ft^2)$ in ASCE 7-16 [1]. This change agrees well with the results of the present study, at which the minimum area-averaged peak pressure coefficient was found on areas much greater than $9.2\ m^2$ $(100\ ft^2)$. For example, the minimum area-averaged peak pressure coefficient occurs on a tributary area of $24\ m^2$ in the corner zone of the 10 m high building.

Ultimately, the advantage of having the minimum peak assigned for a tributary area of $46\ m^2$ $(500\ ft^2)$ in the curve of the area-averaged peak pressure coefficients in the Canadian code and the American standard is clear by observing the experimental area-averaged peaks on the corner zone in Fig. 18 and 19.

The curve of peak pressure coefficients in ASCE 7-10 [2] and NBCC 2015 [28] would cover all the experimental results if the minimum value of peak pressure coefficients would have shifted to the right until it corresponds to a tributary area of $46\ m^2$ $(500\ ft^2)$.

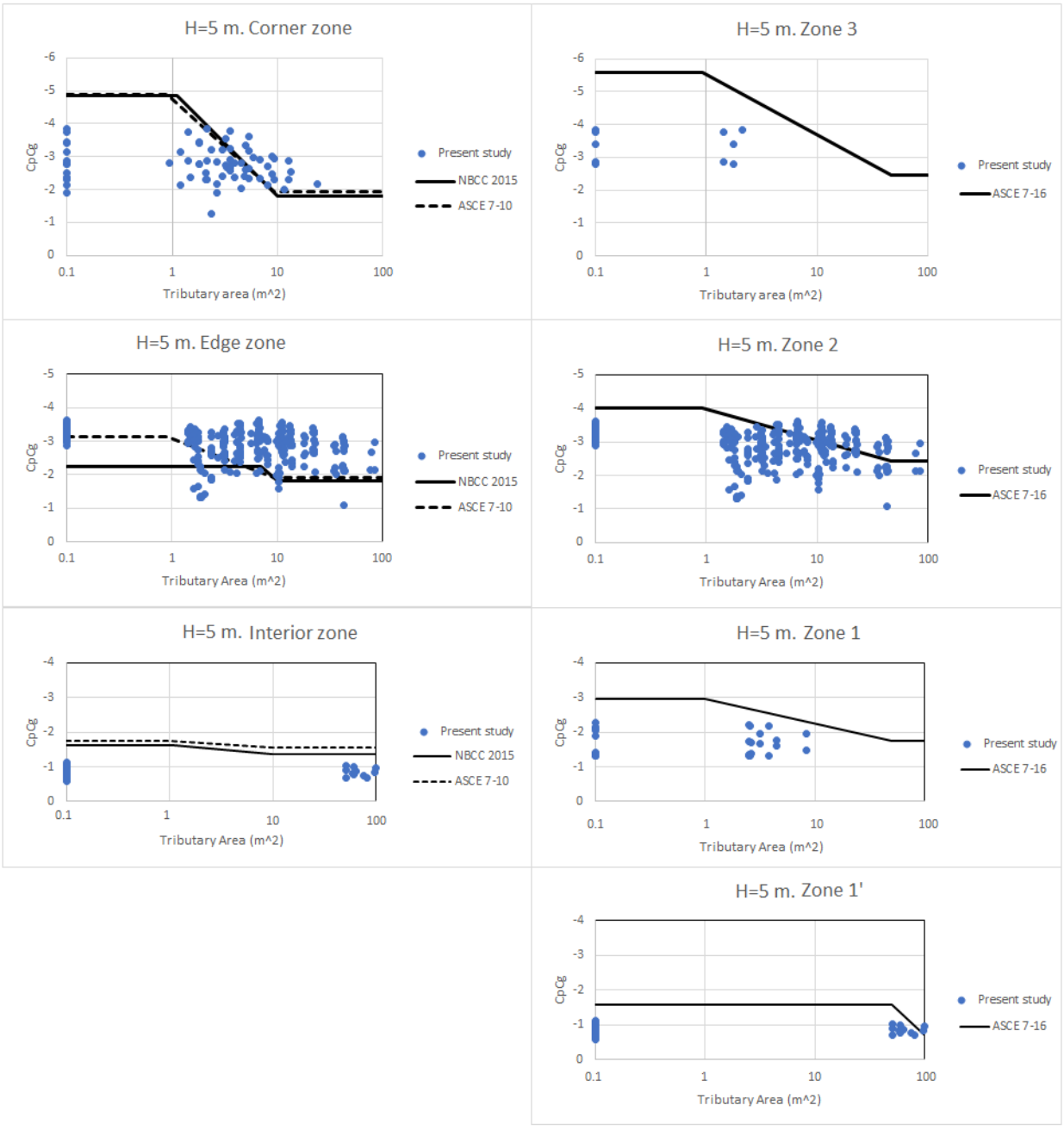

Figure 18: Comparison of the most critical local and area-averaged peak pressure coefficients, CpCg, of the present study and the values recommended by the American standards and the Canadian code (H = 5 m, Exposure C).

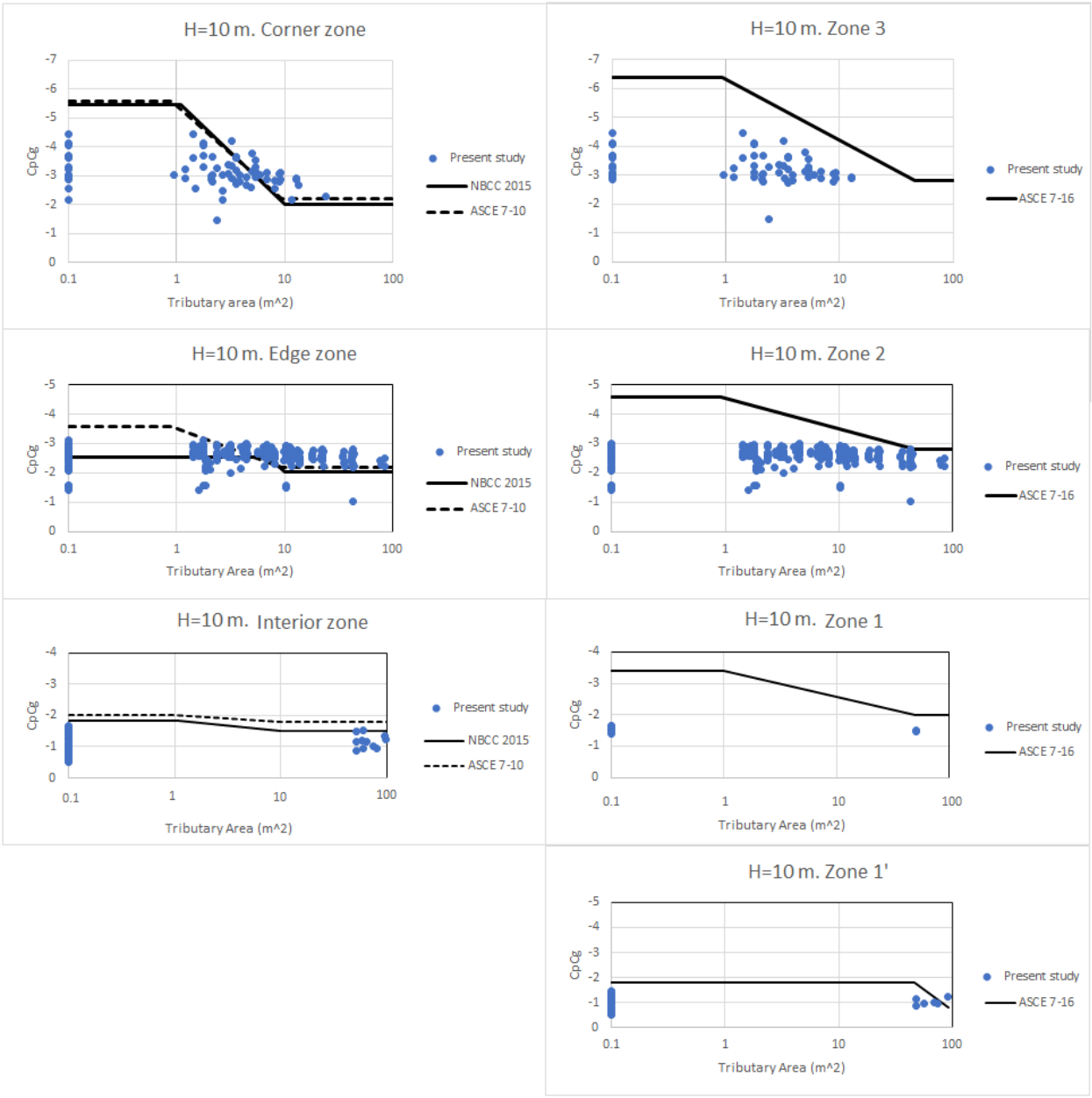

Figure 19: Comparison of the most critical local and area-averaged peak pressure coefficients, CpCg, of the present study and the values recommended by the American standards and the Canadian code (H = 10 m, Exposure C).

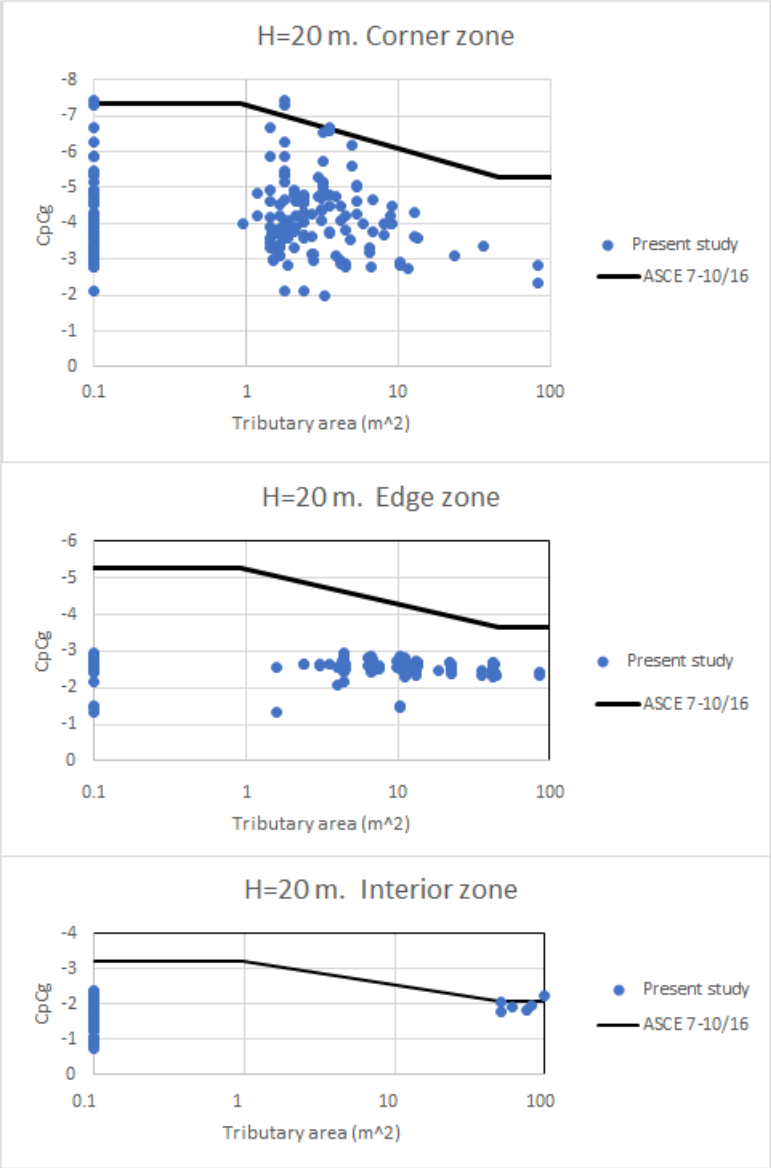

Figure 20: Comparison of the most critical local and area-averaged peak pressure coefficients, CpCg, of the present study and the values recommended by ASCE 7-10/16 (H = 20 m, Exposure C).

7.2 Roof pressure zones

Comparison of the present study with the roof zonal systems of the North American codes and standards can be accomplished by setting the pressure zones on the contours of the most critical (enveloped) peak pressure coefficients of the three buildings in the present study. Corner zone should capture the highest peaks in the roof corner and extend to cover an area that is subjected to wind peak pressure coefficients greater than the peak pressure coefficient provided by the code or the standard for the edge zone. On the other hand, the edge zone should not have peaks greater than those specified by the code or the standard

for the edge zone. In these comparisons, peak pressure coefficients specified in ASCE 7-10 [2] for the edge zone will be taken as a reference to determine the suitability of the roof zonal systems of the North American codes and standards for the design of large roofs.

Fig. 21 shows the contours of most critical peak pressure coefficients over the bottom-left quarter of the roof for the building of 5 m height in exposure C and exposure B, as well as, the pressure zones of the three codes and standards. As shown, corner zones of the three codes and standards capture the highest peak pressure coefficients in the roof corner in both exposures, however, the highest peak pressure coefficients developed on the edge zone are approximately the same as those developed on the corner zone, which are greater than the edge zone peak pressure coefficients of ASCE 7-10 [2] for the 5 m high building in both exposures. In this case, corner and edge zones should be treated as a single pressure zone with the same peak pressure coefficients. Again, this will be very costly for large buildings, however, it is safe.

The pressure zones of ASCE 7-10 [2], NBCC 2015 [28] and ASCE 7-16 [1]; and the contours of most critical pressure coefficients for the building of 10 m height in exposure C and exposure B are presented in Fig. 22. According to ASCE 7-10 [2], the maximum peak pressure coefficient for the edge zone and for the 10 m high building in exposure C is -3.6, the corner zone size of NBCC 2015 [28] and ASCE 7-10 [2] is adequate to capture the wind peak pressure coefficients higher than -3.6, whereas the corner zone of ASCE 7-16 [1] is slightly oversized along the leading edges. It should be noted that the L-shaped corner zone of ASCE 7-16 [1] takes the same spatial distribution of the high peaks in the roof corner; however, it extends a bit more along the leading edge, and captures peak pressure coefficients lower than the value provided by ASCE 7-10 [2] for the edge zone. The same scenario applies to the wind load distribution in exposure B, where the corresponding value of the edge zone peak pressure coefficient in ASCE 7-10 [2] for exposure B is equal to -5.1. As shown in the figure, the corner zone of ASCE 7-10 [2] and NBCC 2015 [28] includes all pressure coefficients greater than -5, and the corner zone of ASCE 7-16 [1] extends along the leading edge and captures relatively low-pressure coefficients. As a result, the proper corner zone for such buildings of around 10 m height should be sized according to NBCC 2015 [28] or ASCE 7-10 [2] and shaped based on ASCE 7-16 [1] as will be shown clearly in Fig. 24.

Fig. 23 shows contours of most critical peak pressure coefficients for the 20 m high building in exposure C and Exposure B; and the pressure zones of ASCE 7-16 [1], ASCE 7-10 [2] and NBCC 2015 [28] based on the provisions of mid-rise buildings. The corner zone is very large such that it extends along the leading edge to include wind peak pressure coefficients much lower than those specified for the edge zone in ASCE 7-10 [2] for both exposures (-5.2 for exposure C and -4 for exposure B).

Experimental examination of wind loads on the buildings of 5 m and 10 m heights results in two different scenarios: similar peak pressure coefficients occur in the corner and the edge zone for the 5 m high building, and the L-shaped distribution of high wind pressures in the roof corner for the 10 m high building. However, each scenario should be generalized for a set of heights rather than a specific height, for this reason, an intermediate height of 8 m (26 ft) may be selected to separate between the two scenarios. Fig. 24 presents proposed roof zonal systems for large low-slope roofs of low-rise buildings. The proposed roof zones are based on the experimental results of the present study. For height greater or equal to 8 m, Fig. 24 (a) suggests 3 zones: L-shaped corner, edge, and interior zones, while for height less than 8 m, the corner and edge zones are treated as a single zone (exterior zone) as shown in Fig. 24 (b). The size of the long side of the L-shaped corner is the end-zone width, z, while the short side size is z/3 and it is specified based on the experimental data for both C and B exposures.

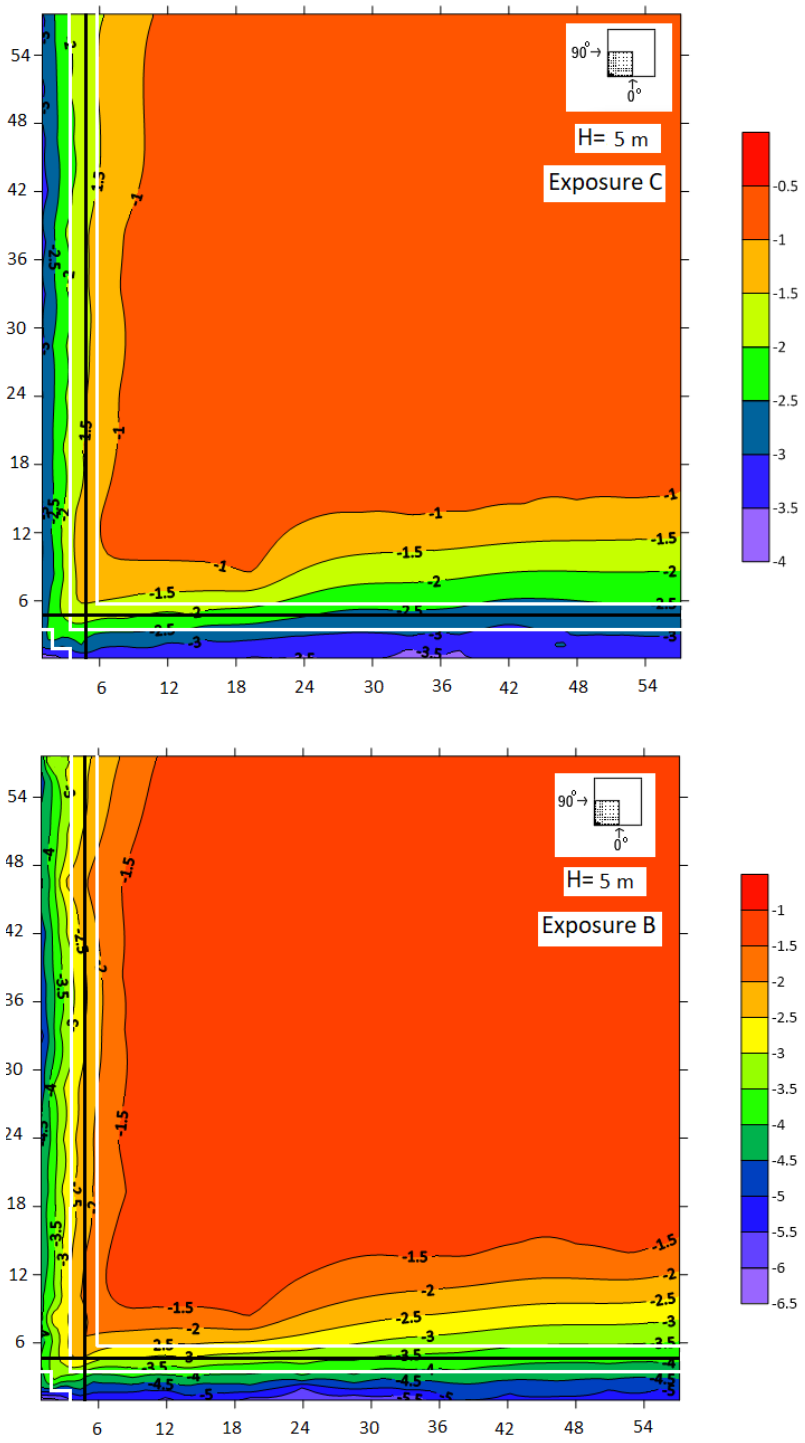

Figure 21: Contours of most critical peak pressure coefficients, CpCg, for the building of 5 m height in exposure C and exposure B, with the pressure zones of ASCE 7-16 [1] (white lines), NBCC 2015 [28] and ASCE 7-10 [2] (black lines).

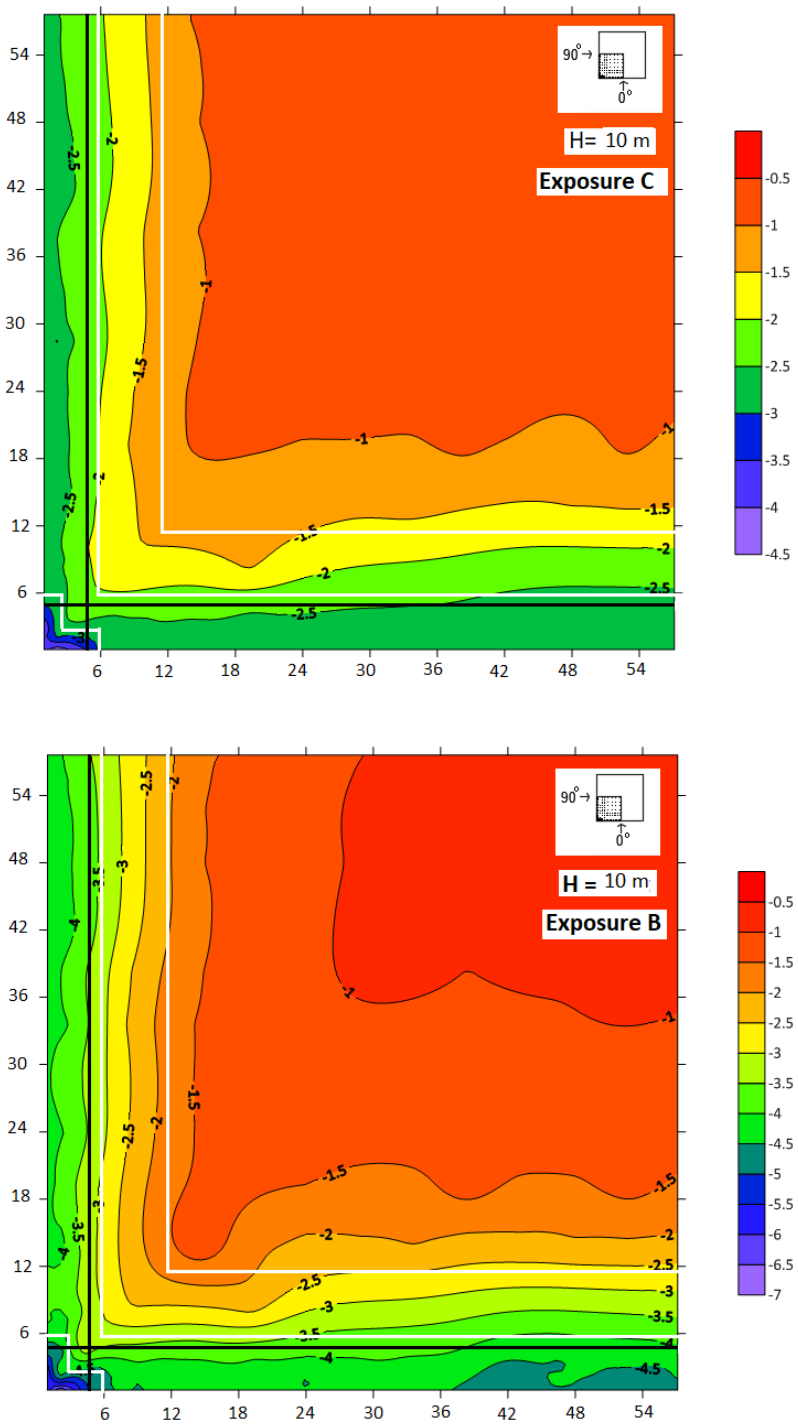

Figure 22: Contours of most critical peak pressure coefficients, CpCg, for the building of 10 m height in exposure C and exposure B, with the pressure zones of ASCE 7-16 [1] (white lines), NBCC 2015 [28] and ASCE 7-10 [2] (black lines).

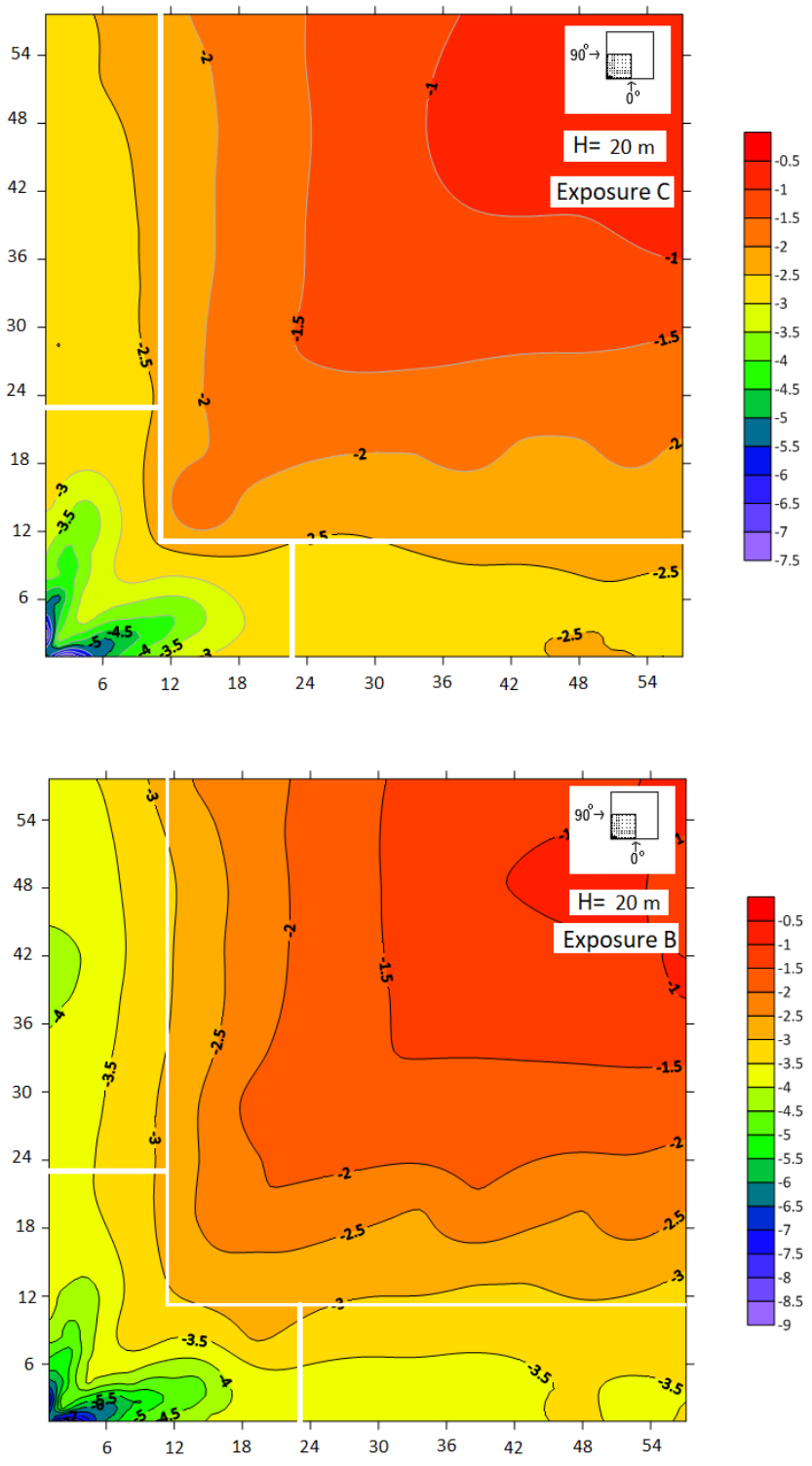

Figure 23: Contours of most critical peak pressure coefficients, CpCg, for the building of 20 m height in exposure C and Exposure B, with the pressure zones of ASCE 7-16 [1], NBCC 2015 [28] and ASCE 7-10 [2].

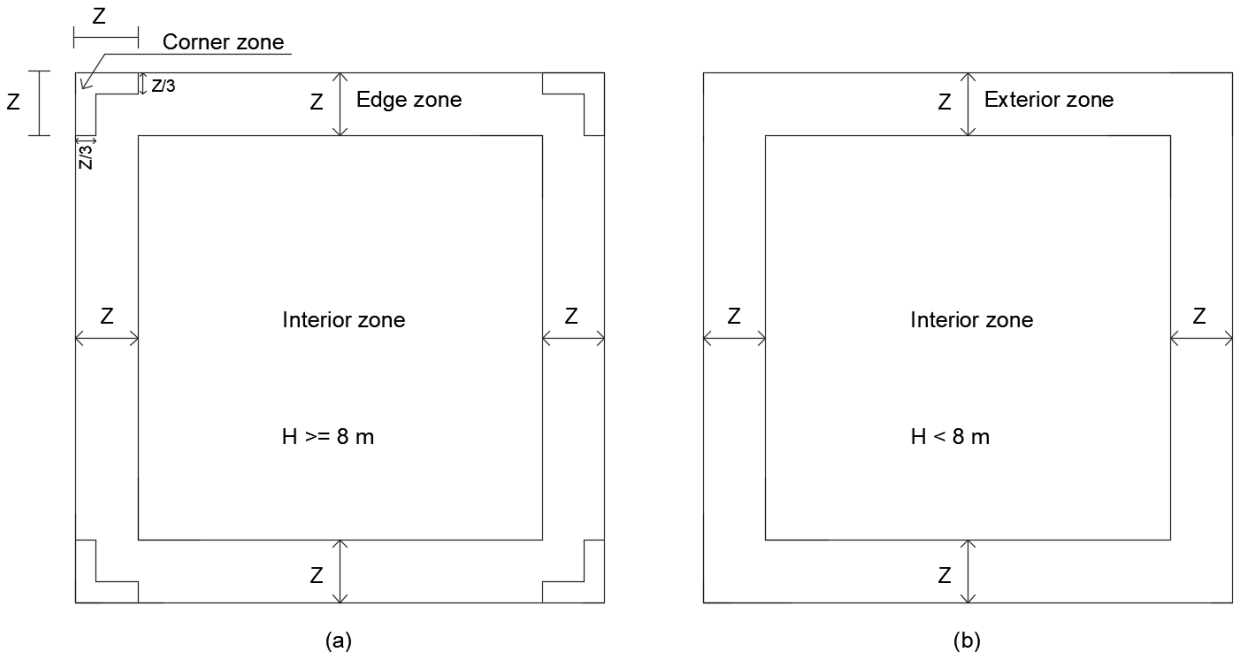

Figure 24: Proposed zonal system for low-slope low-rise buildings of large geometries, (a) height greater or equal to 8 m, (b) height less than 8 m (z is the end-zone width defined in NBCC 2015 [28]).

8 Concluding remarks

This study investigated wind loads on low-slope (less than < 7°) roof buildings of large plan dimensions (larger than 60 m (200 ft)) to investigate the applicability of the North American codes and standards to such buildings. The main findings of the study can be summarized as follows:

1. Peak pressure coefficients recommended by ASCE 7-16 [1] for low-slope roofs are much higher than the actual wind loads on large low-slope roofs of low-rise buildings - using these provisions for large low-slope roof design is uneconomical.

2. Peak pressure coefficients of ASCE 7-10 [2] specified for low-slope roofs are conservative and economical for large low-slope roof design.

3. Peak pressure coefficients of NBCC 2015 [28] recommended for low-slope roofs are also applicable to large low-slope roofs except the peak pressure coefficients provided for the edge zone for which an increase has been recommended.

4. For large low-slope roof low-rise buildings of height less than 8 m, wind loads developed on the corner zone and the edge zone are comparable.

5. For large low-slope roof low-rise buildings of height of 8 m or more, the distribution of high pressures on the corner zone takes an L-shape.

6. Area-averaged wind loads on the edge zone of large roofs decrease marginally as the tributary area increases.

7. The spatial distribution of wind pressures over large roofs is similar in both open country and suburban exposures.

Based on the experimental findings and for large low-slope roof low-rise buildings, it is recommended to treat the corner and the edge zones as a single zone for buildings of height less than 8 m and to define the corner zone as an L-shape for buildings higher or equal to 8 m. Also, the peak pressure coefficients provided by NBCC 2015 [28] for the edge zone are low and should be increased to match those provided by ASCE 7-10 [2].

Acknowledgements

This study was supported financially by the Natural Sciences and Engineering Research Council of Canada (NSERC). The financial support is gratefully acknowledged by the authors.

References

[1] ASCE/SEI 7-16. Minimum Design Loads and associated criteria for Buildings and Other Structures. Structural Engineering Institute of ASCE, Reston, VA; 2017.

[2] ASCE/SEI 7-10. Minimum Design Loads for Buildings and Other Structures. Structural Engineering Institute of ASCE, Reston, VA; 2010.

[3] Jensen M. The model-law for phenomena in natural wind. Ingenioren, International edition 2, 1958.

[4] Davenport AG, Isyumov N. The application of the boundary layer wind tunnel to the prediction of wind loading. Proc. Int. Research Seminar on Wind Effects on Buildings and Structures 1967, 201-230.

[5] Akins RE, Cermak JE. Wind pressures on buildings. Technical Report CER 7677REAJEC15, Fluid Dynamics and Diffusion Lab, Colorado State University, Fort Collins, Colo; 1975.

[6] Peterka JA, Cermak JE. Wind pressures on buildings—Probability densities. J Struct Div 1975; 101(6): 1255–1267.

[7] Davenport AG, Surry D, Stathopoulos T. Wind loads on low-rise buildings. Final Report on Phases I and II, BLWT-SS8, University of Western Ontario, London, Ontario, Canada; 1977.

[8] Davenport AG, Surry D, and Stathopoulos T. Wind loads on low-rise buildings. Final Report on Phase III, BLWT-SS4, University of Western Ontario, London, Ontario, Canada; 1978.

[9] Stathopoulos T, Surry D. Scale effects in wind tunnel testing of low buildings. J Wind Eng Ind Aerodyn 1983; 13:313–326.

[10] Stathopoulos T. Wind loads on low-rise buildings – A review of the state of the art. Eng Struct 1984; 6:119–135.

[11] Holmes JD. Wind Loads on Low-rise Buildings-A Review. CSIRO, Division of Building Research, Highett, Victoria, Australia; 1993.

[12] Krishna P. Wind loads on low rise buildings – A review. J Wind Eng Ind Aerodyn 1995; 54–55:383–396.

[13] Kasperski M. Design wind loads for low-rise buildings: a critical review of wind load specifications for industrial buildings. J Wind Eng Ind Aerodyn 1996; 61:169–179.

[14] Uematsu Y, Isyumov N. Wind pressures acting on low-rise buildings. J Wind Eng Ind Aerodyn 1999; 82:1–25.

[15] Stathopoulos T. Wind pressures on flat roof edges and corners. Proc 7th Int Conf on Wind Engineering, Aachen, Germany; 1987.

[16] Cochran LS, Cermak JE. Full-and model-scale cladding pressures on the Texas tech experimental building. J Wind Eng Ind Aerodyn 1992; 43:1589–1600.

[17] Lin JX, Surry D, Tieleman HW. The distribution of pressure near roof corners of flat roof low buildings. J Wind Eng Ind Aerodyn 1995; 56:235–265.

[18] Lin JX, Surry D. The variation of peak loads with tributary area near corners on flat low building roofs. J Wind Eng Ind Aerodyn 1998; 77–78:185–196.

[19] Ho TCE, Surry D, Morrish D, Kopp GA. The UWO contribution to the nist aerodynamic data base for wind on low buildings: Part1. Archiving format and basic aerodynamic data. J Wind Eng Ind Aerodyn 2005; 93:1–30.

[20] St. Pierre LM, Kopp GA, Surry D, Ho TCE. The UWO contribution to the nist aerodynamic database for wind on low buildings: Part2. Comparison of data with wind load provisions. J Wind Eng Ind Aerodyn 2005; 93:31–59.

[21] Oh JH, Kopp GA, Inculet DR. The UWO contribution to the nist aerodynamic database for wind on low buildings: Part3. Internal pressures. J Wind Eng Ind Aerodyn 2007; 95:755–779.

[22] Alrawashdeh H, Stathopoulos T. Wind pressures on large roofs of low buildings and wind codes and standards. J Wind Eng Ind Aerodyn 2015; 147:212–225.

[23] NBC 2010. User's Guide-NBC 2010, Structural Commentaries (Part 4). Issued by the Canadian Commission on Buildings and Fire Codes, National Research Council of Canada; 2010.

[24] EN 1991-1-4. Eurocode 1, 2005: Actions on Structures-General Actions-Part 1-4: Wind Actions, European Standard; 2005.

[25] AS/NZS 1170.2. Australian/New Zealand Standard for Structural Design Actions, part 2: Wind Actions. Sydney, New South Wales, Australia: Standards Australia and Standards New Zealand; 2011.

[26] Mooneghi MA, Irwin P, Chowdhury AG. Partial turbulence simulation method for predicting peak wind loads on small structures and building appurtenances. J Wind Eng Ind Aerodyn 2016; 157: 47-62.

[27] Kopp GA, Morrison MJ. Component and cladding wind loads for low-slope roofs on low-rise buildings. J Struct Eng 2018; 144(4).

[28] NBC 2015. National Building Code of Canada, Volume 1. Issued by the Canadian Commission on Buildings and Fire Codes, National Research Council of Canada; 2015.

[29] NBC 2015. User's Guide-NBC 2015, Structural Commentaries (Commentary I). Issued by the Canadian Commission on Buildings and Fire Codes, National Research Council of Canada; 2015.

[30] Davenport AG. On the assessment of the reliability of wind loading on low buildings. J Wind Eng Ind Aerodyn 1983; 11:21–37.

[31] Stathopoulos T. Wind loads on low buildings: in the wake of Alan Davenport's contribution. J Wind Eng Ind Aerodyn 2003; 91:1565–1585.

[32] Stathopoulos T. Design and fabrication of a wind tunnel for building aero- dynamics. J Wind Eng Ind Aerodyn 1984; 16:361–376.

[33] Ko KP, Chavez M, Baskaran, A. Field monitoring the wind performance of commercial roof (Iowa site) – Part 4. Research Report No. IRC -RR 905; 2018.

[34] ASCE/SEI 49-12. Wind Tunnel Testing for Buildings and Other Structures. Structural Engineering Institute of ASCE, Reston, VA; 2012.

[35] Nakamura Y, Ozono S. The effects of turbulence on a separated and reattaching flow. J. Fluid Mech. 1987; 178: 477-490.

[36] Geurts C.P.W. and Bentum C.V. Wind loading on buildings: Eurocode and experimental approach, in T. Stathopoulos and C.C. Baniotopoulos, Wind Effects on Buildings and Design of Wind- Sensitive Structures, SpringerWeinNewYork 2007; ISBN 978-3-211-73075-1: 31-65.